Supplemental Materials for Maeder et al., "Rapid "open-source" engineering of customized zinc-finger nucleases for highly efficient gene modification"

Supplemental Experimental Procedures

B2H selection media

NM medium has been previously described (Thibodeau-Beganny and Joung, 2007). NM/CCK medium plates contain 100 μg/mL carbenicillin, 30 μg/mL chloramphenicol, 30 μg/mL kanamycin, and 1.5% Bacto-agar.

Construction of zinc finger pools

All master randomized zinc finger libraries were constructed in a standard framework consisting of three tandem repeats of the middle finger of the murine transcription factor Zif268 in which the recognition helix residues have been altered. For each library, recognition helix residues –1, 1, 2, 3, 5, and 6 were randomized using 24 codons (degenerate sequence 5'VNS3') encoding 16 amino acids (excluding cysteine and the aromatics). The theoretical complexity of each library is therefore 24^6= ~2 x 10^8 members. Each library was converted into infectious M13 phage particles as previously described (Joung et al., 2000).

B2H selection strains each harbor: (1) a single copy episome bearing a target site of interest positioned upstream of a promoter which drives co-cistronic expression of two selectable markers (the yeast *HIS3* gene and the bacterial *aadA* gene) and (2) a low copy number plasmid expressing the RNA polymerase α-subunit/yeast Gal4 hybrid protein (α-

Gal4). Strains were constructed as previously described (Thibodeau-Beganny and Joung, 2007). The target binding site of each strain was verified by DNA sequencing.

Zinc finger pools were obtained using two selection steps: In a first step, 10^9 ampicillin-transducing-units (ATU) of randomized zinc finger phage library were introduced into >3 x 10^9 B2H selection strain cells harboring a target subsite of interest. Transformed cells were plated on histidine-deficient NM/CCK medium plates containing 50 μM isopropyl β-d-thiogalactoside (IPTG) and 10 mM 3-aminotriazole (3-AT), a competitive inhibitor of the HIS3 enzyme. After incubation for 24 hours at 37°C followed by 18 hours at room temperature, surviving colonies were scraped from the plates and infected with M13K07 helper phage to rescue the zinc finger-encoding phagemids as infectious phage. In a second step, this enriched phage library was then used to re-infect fresh B2H selection strain cells and the resulting transformants plated on NM/CCK medium plates containing 50 uM IPTG, 10 mM 3-AT, and 20 ug/ml streptomycin. After incubation at 37°C for 48 hours, we inoculated 95 surviving colonies of various sizes into individual wells of a 96-well block containing 1ml of Terrific Broth and 50 μg/ml carbenicillin. These cultures were grown overnight at 37°C and then a 96-pin replicator was used to inoculate a second block of identical cultures. Glycerol was added to a final concentration of 15% to all wells in the first block and this was stored at -80°C. The second block was grown overnight at 37°C and then the 95 cultures were pooled together. Plasmid DNA encoding the finger pools was isolated from 10 ml of the pooled culture using a QIAgen miniprep kit and for many pools a small number of random clones were sequenced with primer OK61. For finger pools against nine subsites, sequencing revealed no strong consensus

(i.e.—the sequences were diverse and did not resemble one another), suggesting that selective pressure for those sites was relatively weak under the initial selection conditions. For each of these nine subsites, the second step of selection was repeated and plated on higher stringency plates to obtain sequences that more closely resembled one another. The higher stringency plates used were NM/CCK medium plates containing 50 μM IPTG, 20 mM 3-AT, and 30 μg/ml streptomycin (for seven subsites: F1 GAT, F2 GAC, F2 GAG, F2 GCG, F2 TGA, F2 TAG, and F2 GTT) or 50 μM IPTG, 25 mM 3-AT, and 40 μg/ml streptomycin (for two subsites: F2 GAA, F2 TGG).

OPEN selections

To create libraries for use in OPEN selections, finger pools were amplified by PCR. For each amplification, first five and then 20 cycles of PCR were performed using the following primers and annealing temperatures (primer names; initial annealing temp; final annealing temp): for finger 1: OK1424 and OK1425; 55°C; 59°C, for finger 2: OK1426 and OK1427; 52°C; 57°C, for finger 3: OK1428 and OK1429; 41°C; 56°C. Amplified individual finger pools were isolated from 10% polyacrylamide gels and fused together by PCR. To do this, equal concentrations of the three finger pool fragments were fused using the following PCR conditions: 94°C, 5 minutes; 10 cycles of 94°C, 30 sec; 50°C, 30 sec; 72°C, 2 min; final extension 72°C, 7 min. This fusion product was purified using a QIAgen PCR purification kit and then amplified by PCR using primers OK1430 and OK1432 with 10 initial cycles of 94°C, 30 sec; 56°C, 30 sec; 72°C, 1 min and 20 additional cycles of 94°C, 30 sec; 64°C, 30 sec; 72°C, 1 min; final extension 72°C, 7 min. The final PCR product (encoding a library of three-finger arrays) was

isolated on a 5% polyacrylamide gel and treated with *Pfu* polymerase and T4 polynucleotide kinase to create overhangs. This fragment was then ligated with *Bbs*I-digested pBR-UV5-GP-FD2 vector backbone which results in a plasmid that expresses the zinc finger array as a FLAG-tagged Gal11P fusion in the B2H system. This ligation was then introduced into *E. coli* XL-1 Blue cells by electroporation and each library was constructed from >3 x 10^6 independent transformants, ensuring at least three-fold oversampling of the theoretical library complexity of ~8.6 x 10^5 (95^3). Libraries were then converted into infectious M13 phage as previously described (Thibodeau-Beganny and Joung, 2007).

All but six (see below) of the OPEN selections were performed in two stages. In the first stage, an OPEN three-finger library was introduced by infection into a B2H selection strain harboring the full target DNA sequence of interest. >2.2 x 10^6 ATU of OPEN phage library (a number which ensures adequate oversampling of the maximal theoretical library diversity) were used to infect >2 x 10^8 B2H selection strain cells and the resulting transformants were plated on two different NM/CCK medium plates containing 50 μM IPTG, 10 mM 3AT, and 20 μg/mL streptomycin or 50 μM IPTG, 25 mM 3AT, and 40 μg/mL streptomycin. After 36-48 hours of incubation, colonies were harvested from the highest stringency plate yielding at least 1000 colonies. These cells were infected with M13K07 helper phage to rescue zinc finger-encoding phagemids, thereby creating an enriched library. In the second stage, 2.5 x 10^6 ATU of this enriched library were used to infect >2 x 10^8 fresh B2H selection strain cells and the resulting transformants plated on a 245x245mm NM/CCK medium plate containing parallel gradients of 3-AT and

streptomycin ranging from 0 mM to 80 mM and 0 μg/mL to 100 μg/mL, respectively. Gradient plates were poured using the method of Szybalski (Bryson and Szybalski, 1952). After incubation at 37°C for a minimum of 48 and a maximum of 96 hours, 12 surviving colonies were picked from the highest stringency edge of the plate and ZFP-encoding plasmids were isolated by plasmid miniprep and sequenced with primer OK61.

For six of the sites we targeted using OPEN, selections were (for historical reasons) performed in a single step instead of two steps. For five sites (EG223L, EG223R, EG292L, EG292R, and EG382L), >3.1 x 10^6 ATU of OPEN phage library were used to infect >4 x 10^8 B2H selection strain cells and the resulting transformants were plated on a series of NM/CCK medium plates containing 50 μM IPTG, 40 mM 3AT, and 60 μg/mL streptomycin, 50 μM IPTG, 60 mM 3AT, and 80μg/mL streptomycin, 0 μM IPTG, 40 mM 3AT, and 60 μg/mL streptomycin or 0 μM IPTG, 60 mM 3AT, and 80 μg/mL streptomycin. For each target site, we picked colonies from the highest stringency plates that yielded colonies. For one site (EG382R), 4.25 x 10^8 ATU of OPEN phage library were used to infect >10^9 B2H selection strain cells and the resulting transformants were plated on a 245x245mm NM/CCK medium plate containing parallel gradients of 3-AT and streptomycin ranging from 0 mM to 80 mM and 0 μg/mL to 100 μg/mL, respectively. Colonies were picked from the highest stringency edge of the plate.

Construction of modularly assembled zinc finger arrays

Modularly assembled zinc finger arrays were assembled using the Zinc Finger Consortium Modular Assembly Kit v1.0 as previously described (Wright et al., 2006).

For each target half-site in the *EGFP* reporter gene, we assembled three-finger arrays using modules from the Barbas, Sangamo, and Toolgen archives but we did not mix and match modules across platforms because: (1) the Barbas group does not suggest use of their modules with others (Mandell and Barbas, 2006), (2) the Toolgen group discovered that their human zinc fingers worked best with one another but not as well with other engineered modules (Bae et al., 2003), and (3) the Sangamo modules were designed to be finger-position-specific and have non-canonical linkers joining them that differ from the TGEKP linker used by the Barbas and Toolgen modules (Liu et al., 2002).

Quantitative bacterial two-hybrid (B2H) assays

Zinc-finger-encoding plasmids identified from OPEN selections were co-transformed with an α-Gal4 expression plasmid into a "B2H reporter strain" harboring a single copy bacterial plasmid with a target binding site positioned upstream of a weak promoter driving *lacZ* expression. B2H reporter strains were constructed as described (Wright et al., 2006). β-galactosidase assays were performed in triplicate as described (Thibodeau et al., 2004).

ZFN expression vectors

All zinc finger arrays were expressed as ZFNs using the Zinc Finger Consortium mammalian expression vector pST1374 (Wright et al., 2006). Zinc finger arrays were excised directly from B2H expression vectors on an *Xba*I/*BamH*I fragment and cloned into pST1374. In this configuration, zinc finger arrays are joined to the *Fok*I nuclease domain by a four amino acid linker of sequence LRGS. We constructed expression

vectors encoding the four-finger *IL2Rγ* ZFNs using amino acid sequences obtained from a previously published study (Miller et al., 2007).

Human cell-based EGFP-disruption assay

Human 293.EGFP cells harbor an integrated retroviral construct which constitutively expresses a β-galactosidase-EGFP fusion protein (Figure 2B). 293.EGFP cells were transfected in triplicate in 24-well plates using calcium phosphate precipitation as previously described (Cathomen et al., 2001). Transfection cocktails included 300 ng each of a CMV promoter-controlled zinc finger nuclease expression vector, 100 ng pDS.RedExpress (Clontech, Mountain view, CA) and pUC118 to 1.5 μg. 600 ng of pRK5.SceI plasmid (Alwin et al., 2005), which expresses the meganuclease I-*Sce*I, was used in place of GFP-ZFN-encoding plasmids for negative controls. 50,000 cells were analyzed by flow cytometry two and five days post-transfection to determine the percentage of EGFP-negative cells. The number of REx-positive cells at day 2 was used to normalize for transfection efficiency. Statistical significance was determined using a two-sided student's t-test with unequal variance.

CEL I nuclease assay for NHEJ-mediated mutation

In this assay, limited-cycle PCR is used to amplify a locus of interest from the genomic DNA of a population of human cells transfected with ZFN expression vectors (Figure 3A). The resulting PCR product is denatured and re-annealed and heteroduplex DNA will form if mutated alleles are present in the population. These DNA fragments can be cleaved at the site of mismatch by the CEL I enzyme into smaller products of predictable

size. Specifically, 2 x 10^6 human Flp-In T-REx 293 cells (Invitrogen) were transfected with pairs of ZFN-encoding plasmids (100 or 250 ng of each ZFN-encoding plasmid) using Lipofectamine 2000 (Invitrogen). Genomic DNA was isolated from nuclease-treated cells at 3 days post-transfection using the QIAgen Blood Mini kit. Limited-cycle PCR (24 cycles) was performed using Platinum PCR SuperMix Hi-Fidelity (Invitrogen) or its equivalent constituent components (Invitrogen) with 50 ng of genomic DNA as template, 8 μCi of each [alpha-^{32}P]-dATP and dCTP, 1 μM each of gene-specific primers (primers OK1681 and OK1682 for *VEGF-A* sites VF2468/VF2471, primers OK1706 and OK1718 for *VEGF-A* sites VF3537/VF3542/VF3552, primers OK1733 and OK1734 for *HoxB13* sites HX508/HX587 or primers OK1736 and OK1738 for *HoxB13* sites HX735/HX761) and 1.25 μl DMSO in a 25 μl reaction volume. PCR products were cleaned up using Sephadex G-50 columns (Roche) and then melted/re-annealed using the following conditions: 95°C for 10 min; 95°C to 85°C cooling at a rate of -2°C/sec; 85°C to 25°C cooling at a rate of -0.1°C/sec; rapid cool to 4°C. Re-annealed PCR products were diluted 1:3.75 in a buffer of 20 mM Tris-HCl (pH 8.8), 2 mM $MgSO_4$, 60 mM KCl, 0.1% Triton X-100 and treated with 1 μl CEL I enzyme (Surveyor nuclease S; Transgenomic) and 1μl Surveyor Enhancer S (Transgenomic) in a 15 μl reaction incubated at 42°C for 20 min. Products were visualized by electrophoresis on a 0.8mm thick, 10% 1X TBE polyacrylamide gel which was dried down and exposed overnight to a phosphorimaging screen. All experiments were performed a minimum of two times.

Gene targeting assays

2 x 10^6 Flp-In T-REx 293 cells were transfected with pairs of plasmids expressing ZFNs (7.5 μg of each ZFN-encoding plasmid) and 50 μg of donor plasmid using nucleofection with solution V and program Q001 (Amaxa). 2 x 10^6 K562 cells were transfected with ZFN expression plasmid pairs (5 or 7.5 μg of each) and matched donor construct (25 or 50 μg donor plasmid) using nucleofection with solution V and program T-16. Genomic DNA was harvested 3 or 4 days post-transfection for 293 or K562 cells, respectively, using a QIAgen Blood Mini kit. Transfection efficiencies were monitored by including a GFP-encoding plasmid in each transfection and determining the percentage of GFP-positive cells by flow cytometry one day post-transfection. For experiments in which cells were arrested in G2 phase, 0.2 μM vinblastine was added 24 hours post-transfection and then removed by washing three times with phosphate buffered saline 14-18 hours later. Limited-cycle PCR assays (24 cycles) were performed using Platinum PCR SuperMix Hi-Fidelity (Invitrogen) or its equivalent constituent components (Invitrogen) with 4 ng genomic DNA, 8 μCi of each [alpha-^{32}P]-dATP and dCTP, 1 μM each of gene-specific primers (OK1776 and OK1777 for *VEGF-A* or OK1845 and OK1846 for *IL2Rγ*) and 1.25 μl DMSO in a 25 μl reaction. Purified PCR product was digested with 25 units *Sal*I or 10 units *BsrB*I restriction enzyme for 2 hours and the resulting products were visualized by electrophoresis on a 10% 1X TBE polyacrylamide gel. This gel was dried down and exposed overnight to a phosphorimaging screen. Quantification of bands was performed using Quantity One software (Bio-Rad).

For Southern blots, 15 μg of genomic DNA (15 μg) was digested with *Msc*I and *Sal*I restriction enzymes for 20 hrs, electrophoresed in 0.8% tris-acetate agarose gels (100 mM Tris-HCl, 10 mM EDTA, pH 8.0 with acetic acid), and transferred to Zeta-probe nylon membrane (BioRad) using 25 mM sodium phosphate (pH 6.5) according to the procedure of Southern (Southern, 1975) as modified for use with the Turbo-Blot downward transfer apparatus (Schleicher & Schuell). The *VEGF*-A DNA probe was generated by PCR amplification of a cloned human *VEGF-A* DNA template using primers OK1823 and OK1824 which was subsequently labeled (25 ng) with [alpha-^{32}P]-dCTP) using Rediprime II random priming reagents (Amersham). Following hybridization (20 hrs) at 65°C in 5 mL ExpressHyb solution (Clontech), the filters were washed with 0.1X SSC/0.1% SDS at 65°C (2 hrs), blotted dry and exposed to a phosphorimager screen and/or film. The filters were scanned in the Typhoon 8600 phosphoimager and relative band intensities were quantified by volume analysis using ImageQuant software (GE Healthcare/Amersham).

Sequencing of modified genomic alleles

The region encompassing each potential ZFN cleavage site was amplified from genomic DNA isolated from populations of human Flp-In T-REx 293 or K562 cells that had been transfected with ZFN expression plasmids alone or with ZFN expression and donor plasmids. PCR conditions for these amplifications were the same as those used for the CEL I (for assessing NHEJ events) or limited-cycle PCR/restriction digest (for assessing gene targeting events) assays but with all components doubled to a final volume of 50μl. CF877 was amplified using primers OK1711 and 1713. PCR reactions were purified

using the QIAgen Minelute PCR Purification kit and eluted with 15 µl 0.1X EB buffer (QIAgen). PCR fragments were cloned into the pCR4Blunt-TOPO plasmid using the Zero Blunt TOPO PCR Cloning Kit for Sequencing (Invitrogen). The TOPO cloning reaction used 4 µl purified PCR product, 1 µl salt solution and 1 µl TOPO vector. 2 µl of TOPO reaction were transformed into One Shot Mach1-T1 chemically competent cells (Invitrogen) or chemically competent Top10 cells (Invitrogen) and plated on LB plates containing 50 µg/ml kanamycin. Plasmid DNAs from transformants were sequenced with a primer designed to bind internal to the PCR product (OK1773 or T3 (Invitrogen) for *VEGF-A*, OS216 for *HoxB13*, M13 primer (Invitrogen) for *CFTR* or OK1838 for *IL2Rγ*.

Tobacco transformation and assay for mutations

The transformation of tobacco protoplasts by electroporation was carried out as previously described (Wright et al., 2005). Plasmids introduced into protoplasts (10 µg each) included those expressing ZFNs that recognize the left (pRW242) and right (pRW246) half sites of target 2163 in *SuRA*. Note that these constructs do not express the heterodimeric variants of *Fok*I endonuclease. Also transformed into protoplasts was a plasmid expressing neomycin phosphotransferase (NPTII) (pDW998). The CaMV 35S promoter was used to drive expression of both the ZFNs and NPTII. Plasmid DNAs were linearized with *BglII* prior to transformation. Protoplasts were allowed to recover and then selected for kanamycin resistance and regenerated into plantlets as previously described (Wright et al., 2005).

DNA was prepared from tissue harvested from individual plantlets using the Epicentre MasterPure Plant Leaf DNA Purification Kit following the manufacturer's directions. An initial PCR screen for mutations at the site of ZFN cleavage was performed using primers DVO4461 and DVO4462 to amplify a 445 bp fragment from both the *SuRA* and *SuRB* loci. PCR was performed with 100 ng of genomic DNA and the following PCR conditions: 94°C 2 min, followed by 34 cycles of 94°C 15 sec, 61°C 15 sec, 72°C 30 sec, and then 72°C for 5 min. The reactions were run out on a 0.8% agarose gel, purified using a QIAgen QIAquick Gel Extraction kit, and sequenced with DVO4462. The resulting sequences were examined for double peaks, which not only indicate sequence differences between *SuRA* and *SuRB*, but also identify potential insertion/deletion events at the ZFN cleavage site in either or both loci.

DNA from candidate mutants was then PCR amplified using a set of nested, allele-specific primers in two consecutive PCR reactions to confirm the mutation and determine if it occurred in *SuRA* or *SuRB*. The primary reaction amplified a 2.15 kb fragment using approximately 100 ng of genomic DNA as template and primers DVO4565 and DVO4461 for *SuRA* and DVO4429 and DVO4461 for *SuRB*. The second PCR reaction amplified a 2 kb fragment using 1 μl of the primary PCR reaction as template and primers DVO4444 and DVO4461 for *SuRA* and DVO4445 and DVO4461 for *SuRB*. All PCR reactions were performed using a Clontech Advantage cDNA Polymerase kit and the following PCR conditions: 94°C 1 min, followed by 34 cycles of 94°C 30 sec, 66°C 30 sec, 68°C 3 min, and then 68°C for 5 min. The reactions were run out on a 0.8% agarose gel, purified with a QIAgen QIAquick Gel Extraction kit and sequenced with primer DVO4462.

ZFN toxicity assays

ZFN expression plasmids and donor templates were transfected into K562 cells using nucleofection as described above. For these experiments, 5 μg of each ZFN expression plasmid, 25 μg of donor, and 15 ng of pmaxGFP (encoding a GFP variant; Amaxa) were included in each transfection. For controls, we transfected: (1) 10 μg of plasmid encoding I-*Sce*I meganuclease (Porteus and Baltimore, 2003) with 25 μg pUC118 and 15 ng of pmaxGFP, (2) 10 μg of plasmid encoding CAD (caspase-activated DNase) protein (Pruett-Miller et al., 2008) with 25 μg pUC118 and 15 ng of pmaxGFP, or (3) 35 μg of pUC118 and 15 ng of pmaxGFP. Cells were assayed for GFP expression at post-transfection days 1 and 7 with a FACScan cytometer. GFP ratios shown in Figure 4D (green bars) were calculated using the formula:

$$\frac{(\%\text{GFP+ in ZFN-transfected cells on day 7} \,/\, \%\text{GFP+ in ZFN-transfected cells on day 1})}{(\%\text{GFP+ in pUC-transfected cells on day 7} \,/\, \%\text{GFP+ in pUC-transfected cells on day 1})}$$

In addition, genomic DNA was harvested using a QIAgen Blood Mini Prep kit on post-transfection days 4 and 7 and assayed for gene targeting using the limited-cycle PCR/restriction digest assay as described above. Gene targeting ratios shown in Figure 4D (purple bars) were calculated by dividing the gene targeting rate on day 7 by the gene targeting rate on day 4. All assays (both GFP and gene targeting) were performed on at least three-independent samples and t-tests of significance were performed by comparing experimentally determined ratios to a fixed ratio value of 1 (i.e.--no change in value). Variant heterodimer *Fok*I domains were constructed by introducing the "+" and "-" mutations (previously described in Miller et al., 2007) into the wild-type *Fok*I nuclease

domain.

Fluorescence in situ hybridization (FISH)

Two-color fluorescence in situ hybridization (FISH) was performed on 3:1 methanol-acetic acid fixed cell lines using bacterial artificial chromosome clones RP11-710L16 (6p21.1; VEGFA) labeled in Spectrum Orange (Abbott-Vysis, Downer's Grove, Il.), or RP11-142P4 (14q31.1; copy number control) labeled in Spectrum Green using standard protocols. Images were captured using an Olympus BX61 fluorescent microscope equipped with a CCD camera, and analysis was performed with Cytovision software (Applied Imaging, San Jose, CA).

Supplemental Figure and Table Legends:

Figure S1 ZiFiT 3.0 -- Web-based software for identifying potential sites targetable by OPEN selection

(A) Screen shot of ZiFiT 3.0 input page. We previously described ZiFiT, a web-based software program that enables users to rapidly identify potential zinc finger nuclease target sites within genes of interest (Sander et al., 2007; Wright et al., 2006). The original implementations of ZiFiT (versions 1.0 and 2.0) were both geared toward making zinc finger nucleases by modular assembly, and the output cross-referenced zinc finger modules available in the Zinc Finger Consortium Modular Assembly Kit 1.0 (Wright et al., 2006). With the implementation of OPEN, we have released ZiFiT Version 3.0, which gives users the option of searching for target sites for which OPEN pools are available. The user pastes a DNA sequence (limited to 10,000 characters) into the text box at the top of the main window. Underneath the main window are three boxes corresponding to finger positions in the zinc finger array. Each box contains a list of the 64 possible nucleotide triplets. By default, triplets are checked for which OPEN pools are currently available from the Zinc Finger Consortium; however, users can manually select or deselect triplet pools to customize their search. Target site composition can be further restricted by options available under the "Advanced/Basic" toggle near the bottom of the screen. By selecting the "Submit" button, the sequence is searched for all target sites using the specified pools and an output is returned.

(B) Screen shot of ZiFiT 3.0 output page. In addition to identifying zinc finger nuclease target sites in the input sequence, it may be desirable to identify matching or highly

similar sites within a genome of interest. ZiFiT Version 3.0 enables the user to BLAST the genome sequence of a desired organism to identify duplicate or related target sites. The BLAST search is implemented by a button link and an organism selection menu provided for each target site returned in the output on the results page. Requests are submitted to the NCBI BLAST servers to provide maximum reliability and speed, and results are typically returned to ZiFiT within a minute. Note that BLAST scoring methods do not identify all matches near the end of a hit if they are separated by mismatches that lower the score of the local alignment. As a result, hits to highly similar target sites lacking information at the ends may need to be analyzed manually.

Figure S2 Schematic of target sites in the *EGFP*, *VEGF-A*, *HoxB13*, and *CFTR* genes

Using ZFNs made by OPEN selections, we targeted (A) five full ZFN sites in the *EGFP* reporter gene (EG223, EG292, EG382, EG502, and EG568), (B) six sites in open chromatin regions of the human *VEGF-A* gene (VF2468, VF2471, VF3537, VF3540, VF3542, and VF3552), (C) five sites in the first coding exon of the human *HoxB13* gene (HX500, HX508, HX587, HX735, and HX761) and one site in the last coding exon of the human *HoxB13* gene (HX2119, not shown), and (D) one site in exon 10 of the human *CFTR* gene (CF877) positioned within 100 base pairs of the ΔF508 deletion.

Figure S3 DNA sequence analysis of endogenous human and plant genes mutagenized by OPEN ZFNs

(A-C) Sequences of (A) *HoxB13* alleles from human 293 cells transfected with HX587 ZFN pair B, (B) *CFTR* alleles from human K562 cells transfected with CF877 ZFNs, and (C) Sequences of *SuRA* alleles from tobacco plants transfected with SR2163 ZFNs (matching sequence from the *SuRB* gene is also shown). Numbers of each allele identified are shown in parentheses. ZFN recognition sites are in bold orange print.

Figure S4 Schematics of donor templates and primers used for gene targeting experiments at the human *VEGF-A* and *IL2Rγ* genes.

Donor templates were constructed for OPEN ZFN pairs that cleave at the VF2468 and VF2471 sites and for a previously described four-finger ZFN pair that cleaves in the *IL2Rγ* gene (Urnov et al., 2005). Each donor template consists of 1.5 kb of genomic DNA sequence centered on the cleavage site and introduces either an 11 bp insertion encoding a *Sal*I restriction site at the center of the cleavage site (for *VEGF-A* targets) or a translationally silent point mutation which creates a *BsrB*I restriction site adjacent to the ZFN cleavage site (for *IL2Rγ*) (Urnov et al., 2005). Arrows indicate primers used for limited-cycle PCR/restriction digest assay described in the text.

Figure S5 Comparison of PCR-based and Southern blot methods for assaying gene targeting efficiencies.

Limited-cycle PCR and Southern blot were used to assess gene targeting efficiencies in cells treated with different ZFNs under various conditions. Dotted red line represents where data points would fall if the two methods were perfectly concordant.

Figure S6 DNA sequence analysis of endogenous human alleles that have undergone gene targeting induced by ZFNs

(A-C) Sequences of alleles sequenced from human K562 cells transfected with (A) VF2468 ZFNs and donor, (B) VF2471 ZFNs and donor, and (C) *IL2Rγ* ZFNs and donor. Data are presented as in Figure S3.

Figure S7 OPEN ZFNs induce stable multi-allelic alterations of at an endogenous human gene

FISH analysis indicated that K562 cells harbor four alleles of the *VEGF-A* gene (A, upper left panel) and we therefore wished to determine how many of these alleles could be altered in a single cell. Limiting dilution cloning was used to isolate single cell clones from two vinblastine-treated K562 cell populations which had undergone high frequencies of gene targeting: 45% and 26% with the VF2468 and VF2471 ZFN pairs, respectively (B, upper panel). (The VF2468 ZFN-treated cells also showed evidence of a 625 bp deletion (blue asterisks), a finding confirmed by sequencing of alleles from these cells (data not shown).) Individual clones from VF2468 ZFN-treated cells harbored no, one, three, or four alleles that had undergone a gene targeting event with some of the

clones also containing the 625 bp deletion (B, lower left panel). Genotype analysis of individual cell clones from the VF2471 ZFN-treated cells revealed clones in which no, one, two, or three *VEGF* alleles had undergone a gene targeting event (B, lower right panel). All individual cell clones were genotyped more than thirty-five days post-transfection, demonstrating that gene targeting events we observed are stably maintained. FISH analysis of three cell clones in which all four *VEGF-A* alleles had undergone the VF2468 ZFN-induced gene targeting event confirmed the continued presence of four copies of *VEGF-A* per cell (A, upper right, and lower left and right panels). FISH was performed with a probe for *VEGF-A* (red) and a control probe for 14q which is present in two copies per cell (green). Taken together, these results demonstrate that OPEN ZFNs can be used to induce permanent alterations in as many as four alleles in a single human cell.

Table S1: Sequences and B2H assays of zinc finger arrays selected by OPEN

The subset of zinc finger arrays we converted to ZFNs for testing in human or plant cells are highlighted in green. As noted in the text, a small number of selections were performed in a single step on plates with fixed concentrations of IPTG, 3-AT, and streptomycin. For these selections, IPTG concentration shown is in μM, 3-AT concentration shown is in mM, and streptomycin concentration shown is in μg/ml. Fold-activation of transcription in the B2H system was determined by comparing *lacZ* expression from B2H reporter strains harboring a zinc finger array (fused to a fragment of the yeast Gal11P protein) to matched strains harboring a control that does not express a zinc finger array. All determinations were performed in triplicate and the means and

standard deviations of these means are shown. Certain target sites cause a higher basal level of *lacZ* expression in the quantitative B2H assay and the finger arrays tested on these sites may exhibit lower apparent fold-activations due to this effect (affected values are highlighted in yellow). Certain zinc finger arrays (marked by a "+" in the last column) harbor additional mutations outside of the three randomized recognition helices that were most likely introduced during library construction. The identities of these various mutations are available upon request.

Although half-site EG502L did not yield OPEN zinc-finger arrays which activated by more than three-fold, we note that the basal level of transcription from the B2H reporter bearing this site was high, a situation which can artifactually lower the apparent fold-activation observed.

25 of the 28 OPEN selections we performed for the human *VEGF-A*, human *HoxB13*, human *CFTR*, and tobacco *SuRA* genes yielded zinc-finger arrays whose sequences closely resembled one another. However, one of these 25 selections (for half-site VF3540R) yielded fingers with sequences that appeared to bind to an alternative site (discussed below). For 22 of the other 24 selections, we obtained at least one zinc-finger array which activated *lacZ* expression by more than three-fold in the quantitative B2H assay. The two remaining selections were also deemed to be successful because their reporters possessed a high basal level of transcription which can artifactually mask a higher true fold-activation. For one selection (site VF3540R), examination of the recognition helix sequences of the arrays obtained from OPEN selection suggests that

these finger arrays do not bind to the intended nine base pair site but rather to the site that is shifted 3' in register by 1 bp (i.e.--these arrays bind to the site: 5'-GCG GCG GAC-3' instead of 5'-GGC GGC GGA-3'). For example, for finger 1, the Asp and Glu selected at position -1 and the Asn selected at position 3 of the recognition helix would be expected to specify cytosine and adenine, respectively, and not the adenine and guanine actually present in the subsite. Similarly, for finger 3, the Arg selected at position -1 and the Ser and Asp selected at position 3 of the recognition helix would be expected to specify guanine and cytosine, respectively, and not the cytosine and guanine actually present. Thus, this selection was deemed to be unsuccessful.

Table S2 ZFN target sites and associated zinc-finger arrays and ZFNs

All target sites and half-sites shown are written 5' to 3'. Names of zinc-finger arrays are the same as in Table S1.

Table S3: Primers used in this study

Supplemental References:

Alwin, S., Gere, M. B., Guhl, E., Effertz, K., Barbas, C. F., 3rd, Segal, D. J., Weitzman, M. D., and Cathomen, T. (2005). Custom zinc-finger nucleases for use in human cells. Mol Ther *12*, 610-617.

Bae, K. H., Do Kwon, Y., Shin, H. C., Hwang, M. S., Ryu, E. H., Park, K. S., Yang, H. Y., Lee, D. K., Lee, Y., Park, J.*, et al.* (2003). Human zinc fingers as building blocks in the construction of artificial transcription factors. Nat Biotechnol *21*, 275-280.

Bryson, V., and Szybalski, W. (1952). Microbial Selection. Science *116*, 45-51.

Cathomen, T., Stracker, T. H., Gilbert, L. B., and Weitzman, M. D. (2001). A genetic screen identifies a cellular regulator of adeno-associated virus. Proc Natl Acad Sci U S A *98*, 14991-14996.

Joung, J. K., Ramm, E. I., and Pabo, C. O. (2000). A bacterial two-hybrid selection system for studying protein-DNA and protein-protein interactions. Proc Natl Acad Sci U S A *97*, 7382-7387.

Liu, Q., Xia, Z., Zhong, X., and Case, C. C. (2002). Validated zinc finger protein designs for all 16 GNN DNA triplet targets. J Biol Chem *277*, 3850-3856.

Mandell, J. G., and Barbas, C. F., 3rd (2006). Zinc Finger Tools: custom DNA-binding domains for transcription factors and nucleases. Nucleic Acids Res *34*, W516-523.

Miller, J. C., Holmes, M. C., Wang, J., Guschin, D. Y., Lee, Y. L., Rupniewski, I., Beausejour, C. M., Waite, A. J., Wang, N. S., Kim, K. A.*, et al.* (2007). An improved zinc-finger nuclease architecture for highly specific genome editing. Nat Biotechnol *25*, 778-785.

Porteus, M. H., and Baltimore, D. (2003). Chimeric nucleases stimulate gene targeting in human cells. Science *300*, 763.

Pruett-Miller, S. M., Connelly, J. P., Maeder, M. L., Joung, J. K., and Porteus, M. H. (2008). Comparison of Zinc Finger Nucleases for Use in Gene Targeting in Mammalian Cells. Molecular Therapy, doi: 10.1038/mt.2008.1020.

Sander, J. D., Zaback, P., Joung, J. K., Voytas, D. F., and Dobbs, D. (2007). Zinc Finger Targeter (ZiFiT): an engineered zinc finger/target site design tool. Nucleic Acids Res *35*, W599-605.

Southern, E. M. (1975). Detection of specific sequences among DNA fragments separated by gel electrophoresis. J Mol Biol *98*, 503-517.

Thibodeau, S. A., Fang, R., and Joung, J. K. (2004). High-throughput beta-galactosidase assay for bacterial cell-based reporter systems. Biotechniques *36*, 410-415.

Thibodeau-Beganny, S., and Joung, J. K. (2007). Engineering Cys2His2 Zinc Finger Domains Using a Bacterial Cell-Based Two-Hybrid Selection System. Methods in Molecular Biology *408*, 317-334.

Urnov, F. D., Miller, J. C., Lee, Y. L., Beausejour, C. M., Rock, J. M., Augustus, S., Jamieson, A. C., Porteus, M. H., Gregory, P. D., and Holmes, M. C. (2005). Highly efficient endogenous human gene correction using designed zinc-finger nucleases. Nature *435*, 646-651.

Wright, D. A., Thibodeau-Beganny, S., Sander, J. D., Winfrey, R. J., Hirsh, A. S., Eichtinger, M., Fu, F., Porteus, M. H., Dobbs, D., Voytas, D. F., and Joung, J. K. (2006). Standardized reagents and protocols for engineering zinc finger nucleases by modular assembly. Nat Protoc *1*, 1637-1652.

Wright, D. A., Townsend, J. A., Winfrey, R. J., Jr., Irwin, P. A., Rajagopal, J., Lonosky, P. M., Hall, B. D., Jondle, M. D., and Voytas, D. F. (2005). High-frequency homologous recombination in plants mediated by zinc-finger nucleases. Plant J *44*, 693-705.

Figure S1 ZiFiT 3.0 -- Web-based software for identifying potential sites targetable by OPEN selection

A.

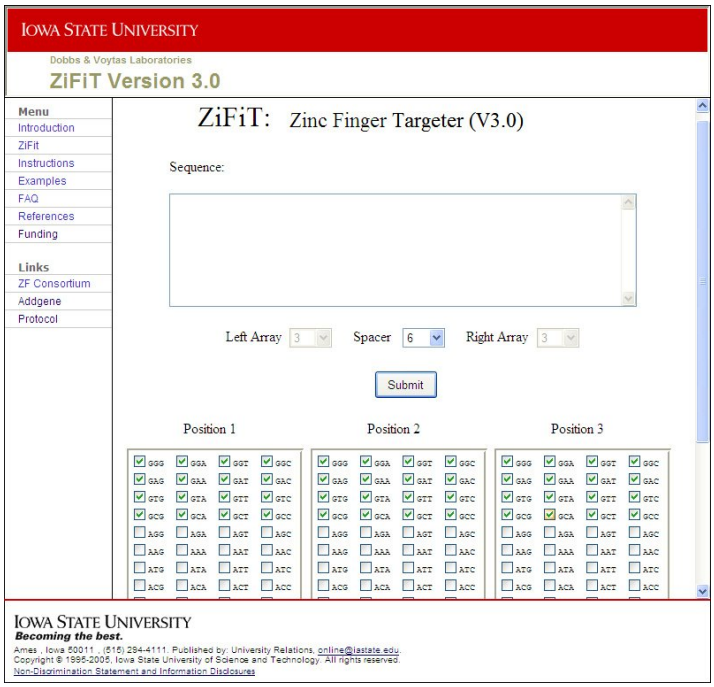

B.

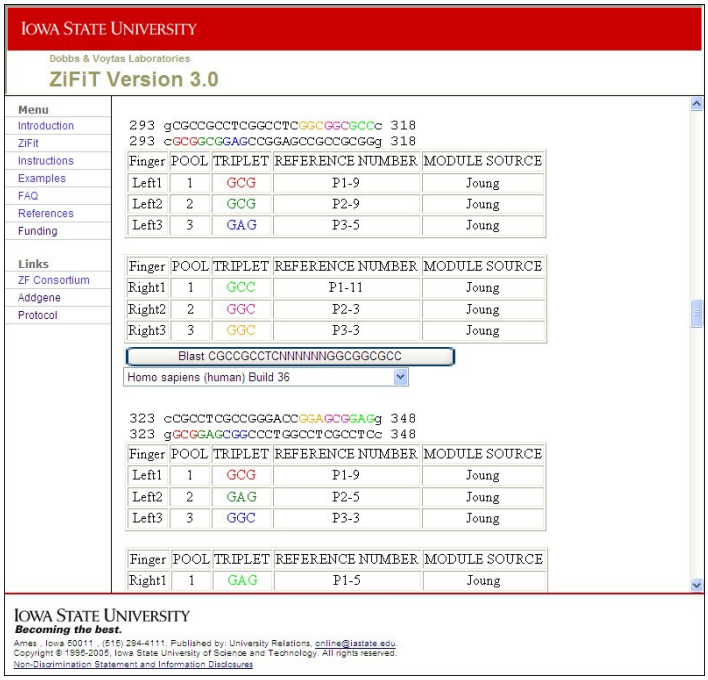

Figure S2 Schematic of target sites in the *EGFP*, *VEGF-A*, *HoxB13*, and *CFTR* genes

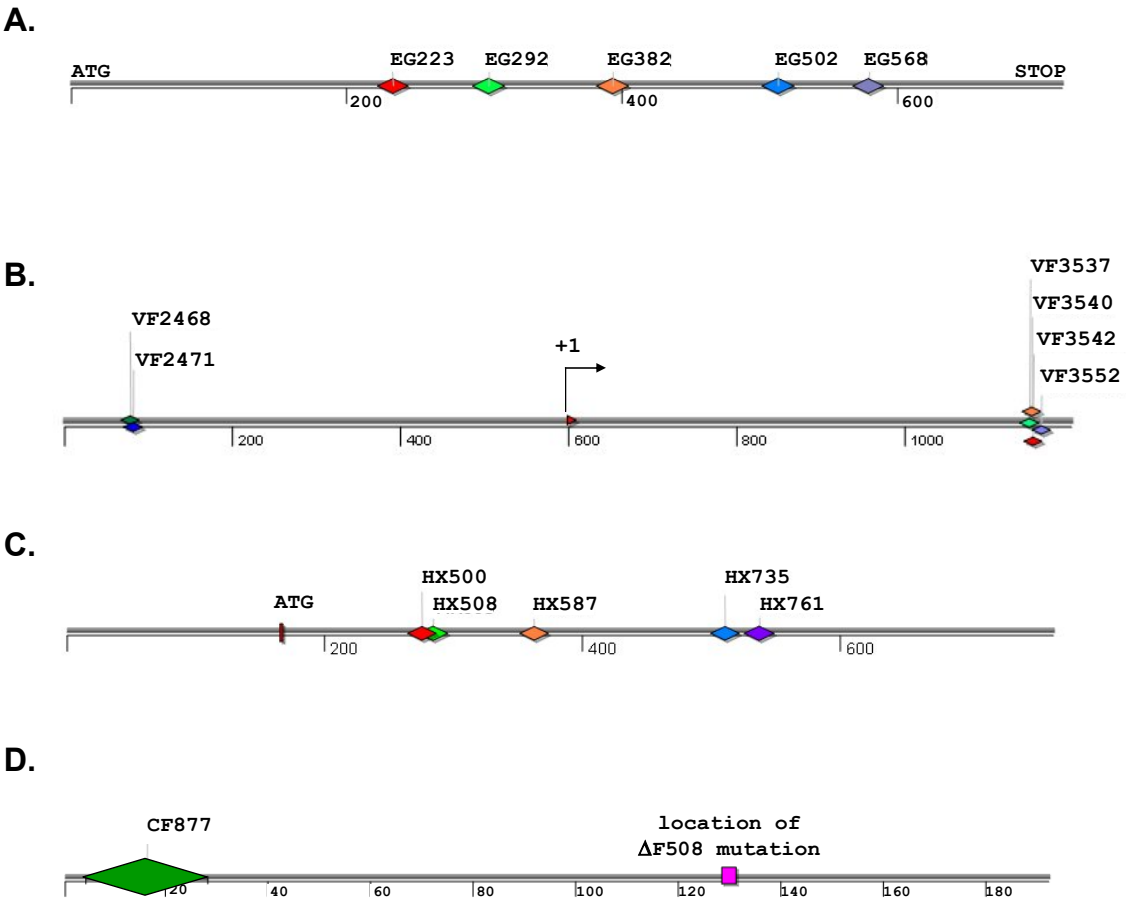

Figure S3 DNA sequence analysis of endogenous human and plant genes mutagenized by OPEN ZFNs

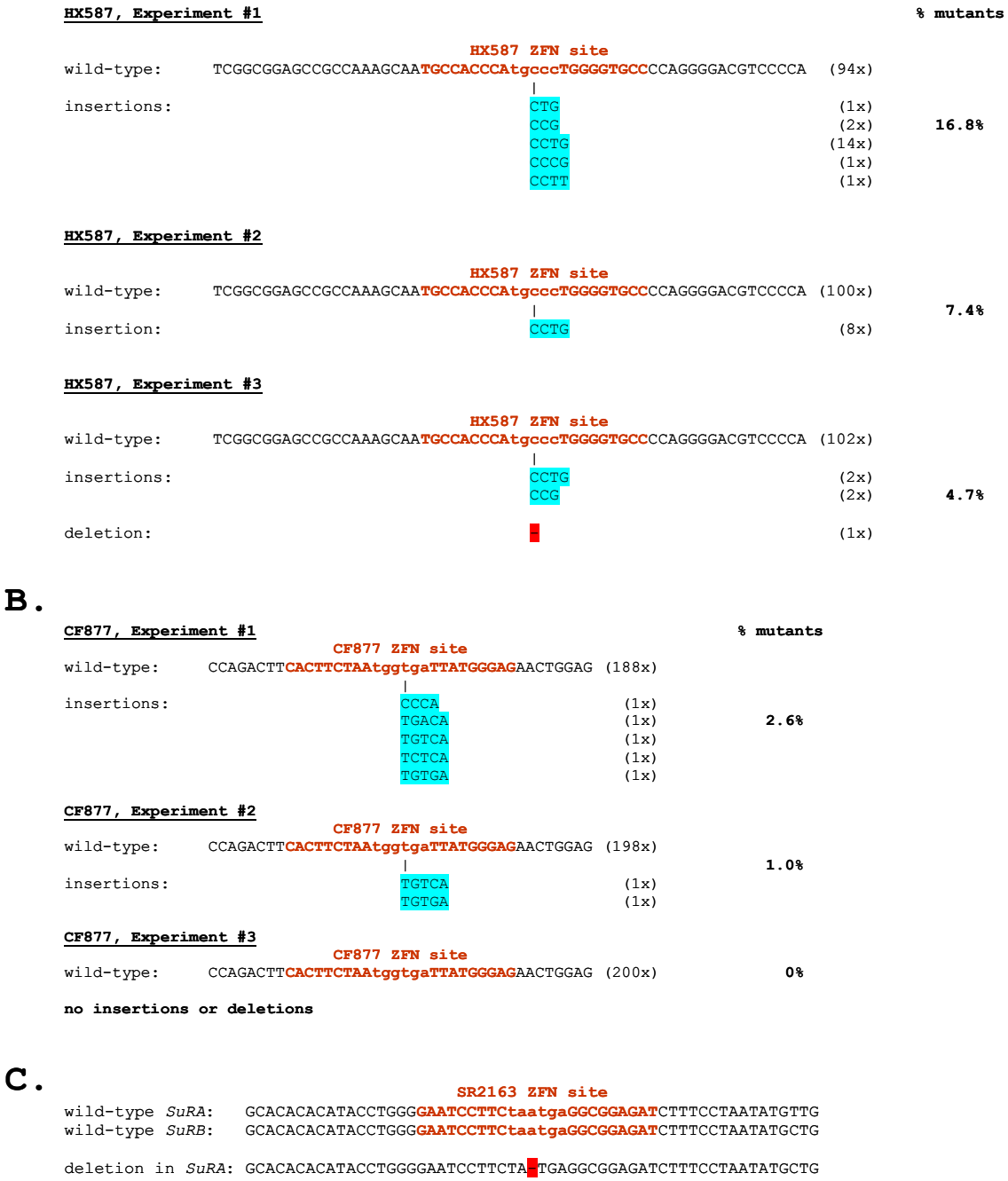

Figure S4 Schematics of donor templates and primers used for gene targeting experiments at the human *VEGF-A* and *IL2Rγ* genes.

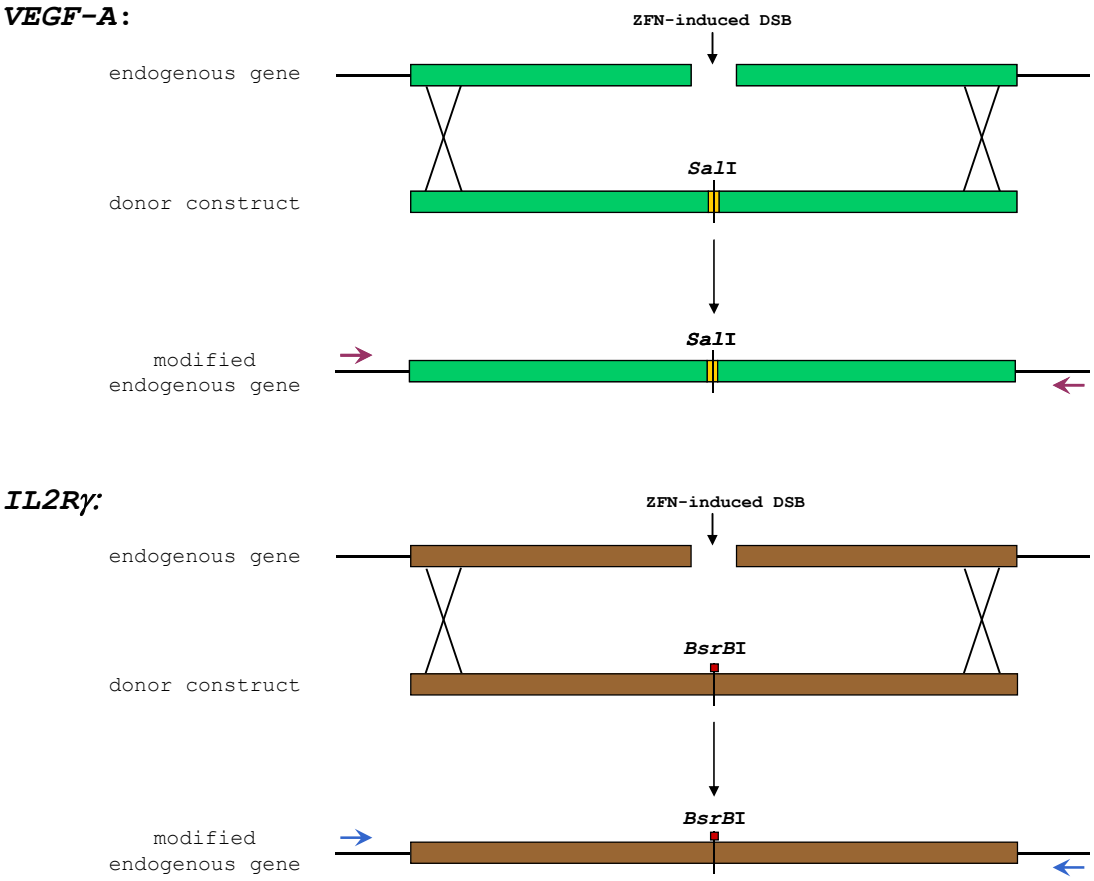

Figure S5 Comparison of PCR-based and Southern blot methods for assaying gene targeting efficiencies

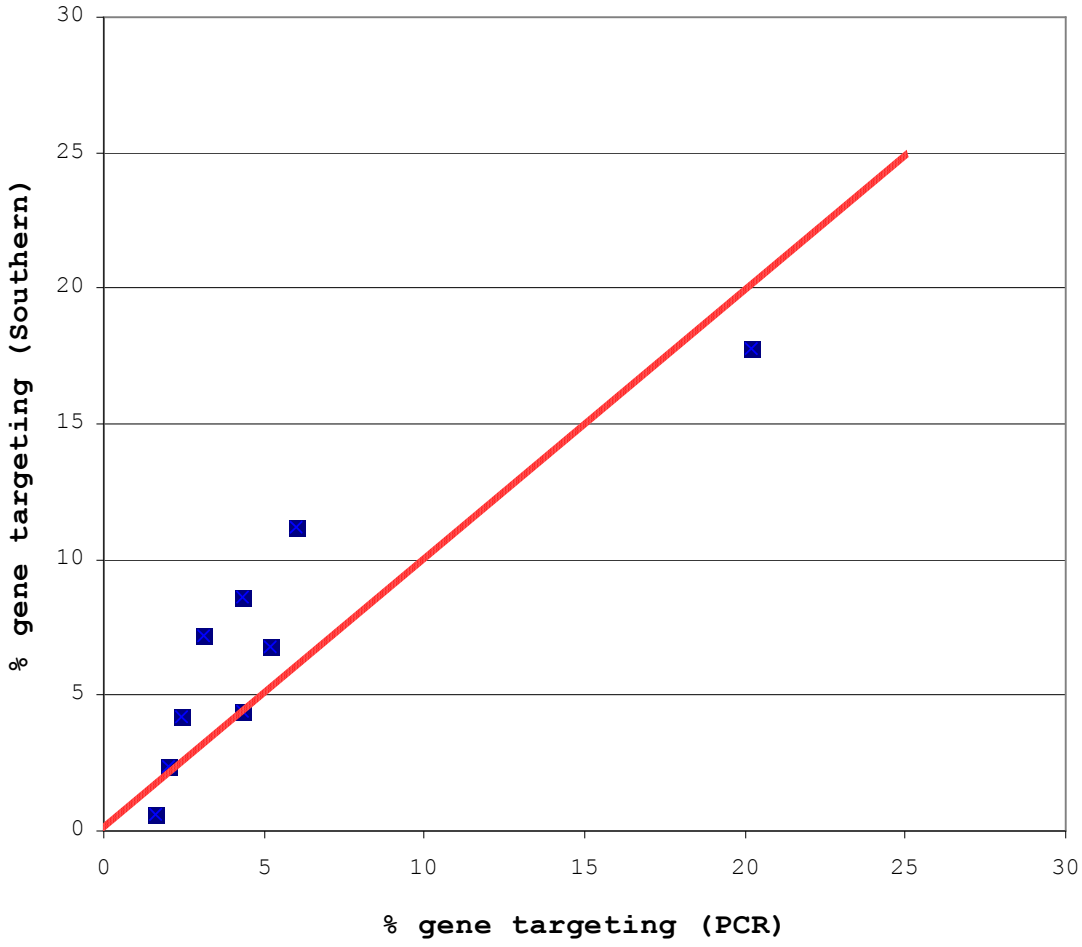

Figure S6 DNA sequence analysis of endogenous human alleles that have undergone gene targeting induced by ZFNs

A.

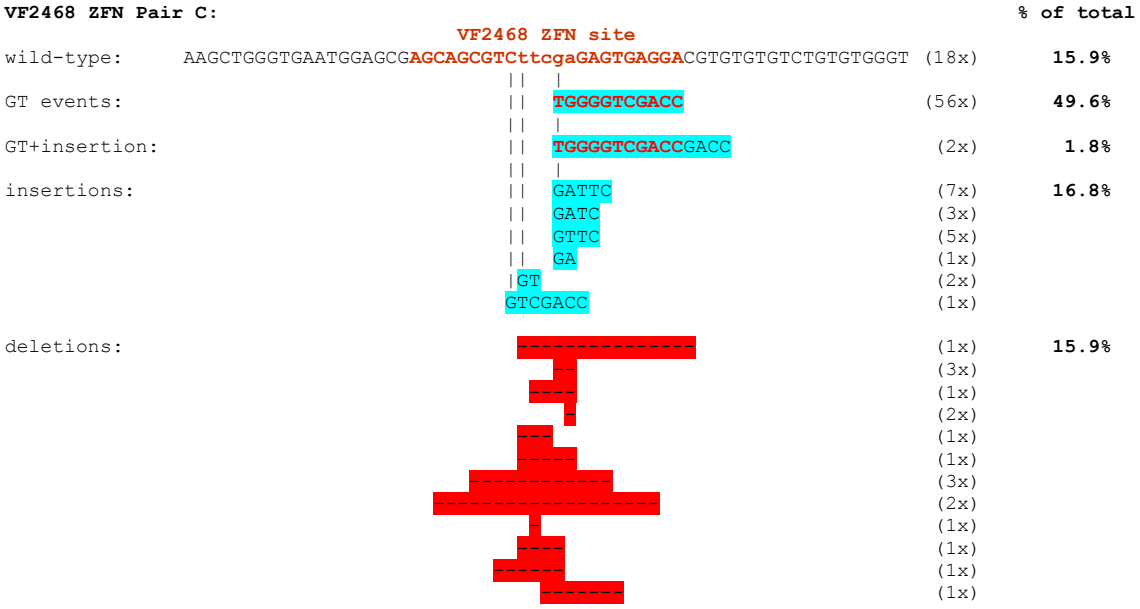

B.

C.


IL2Rγ ZFN pair:
% of total
IL2Rγ ZFN site
wild-type: CACGTTTCGTGTTCGGAGCCGCTTTaacccACTCTGTGGAAGTGCTCAGCATTGGAGTGAATG (39x) 32.0%
GT events: G (31x) 25.4%
GT+insertion: CCCAAcccG (11x) 9.0%
IL2Rγ ZFN site
wild-type: CACGTTTCGTGTTCGGAGCCGCTTTaacccACTCTGTGGAAGTGCTCAGCATTGGAGTGAATG
insertions: CCGA (1x)
CCCAA (26x) 24.6%
CCAA (3x)
deletions: (1x) 9.0%
(1x)
(2x)
518 bp deletion (2x)
(1x)
(1x)
(2x)
(1x)

Figure S7 (part 1 of 2)

A.

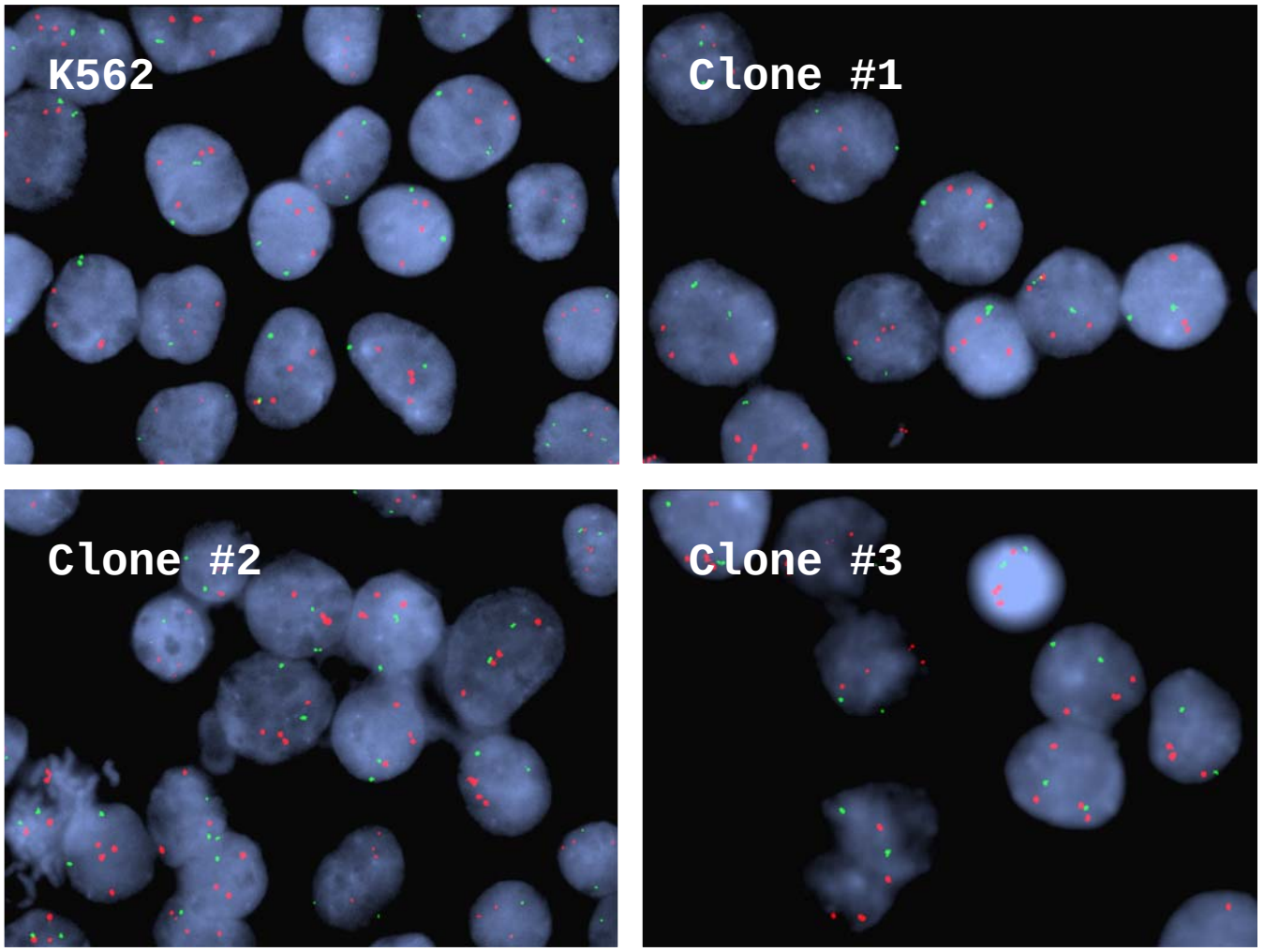

Figure S7 (part 2 of 2)

B.

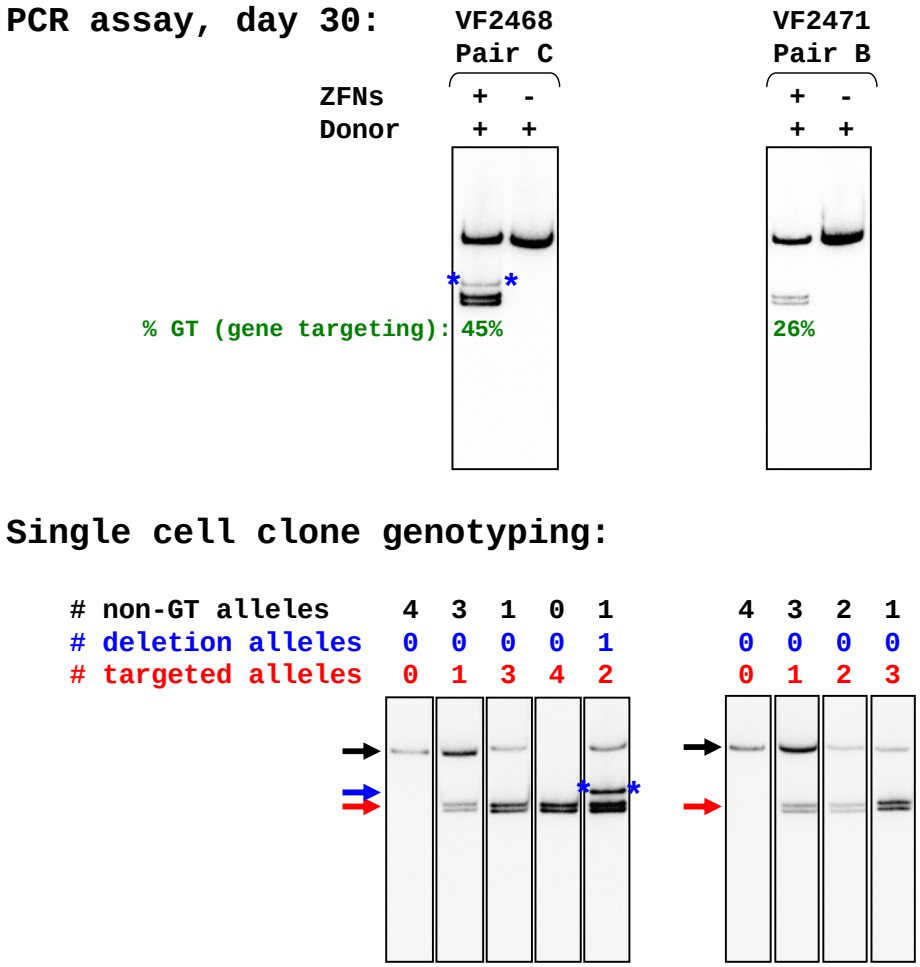

Table S1

Table S1: Sequences and B2H assays of zinc finger arrays selected by OPEN								
ZFN Name	**Site Name**	**Selection conditions (IPTG/3-AT/Strep)**	**F1 subsite/RH sequence**	**F2 subsite/RH sequence**	**F3 subsite/RH sequence**	**Mean B2H fold-activation**	**S.D. of B2H fold-activation**	**Other mutations (of unknown significance) present?**
			GTA	GGG	GTC			
OZ001	EG223L	50/40/60	QDSSLRR	RQEHLVR	DPTSLNR	4.24	0.17	
OZ002	EG223L	50/40/60	QQSSLLR	RQEHLVR	DPTSLNR	3.50	0.13	
OZ003	EG223L	50/40/60	QPSSLTR	RKPHLVN	QPTSLQL	0.79	0.03	
OZ004	EG223L	50/40/60	QQSSLLR	RGEHLTR	DQTVLRR	3.50	0.33	
OZ005	EG223L	50/40/60	QQSSLLR	RGEHLTR	EPTSLIR	3.17	2.10	
OZ006	EG223L	50/40/60	QPSSLTR	RREHLVS	DRRPLPR	1.74	0.65	
OZ007	EG223L	0/40/60	QGSALAR	RREHLVR	DPTSLNR	4.09	0.08	
OZ008	EG223L	0/40/60	QSSSLTR	RGEHLTR	ESGALRR	2.57	1.15	
OZ009	EG223L	0/40/60	QASALSR	RREHLVR	ESGALRR	5.23	0.94	
OZ010	EG223L	0/40/60	QSQALVR	RVEHLNN	DRTSLPR	0.76	0.09	
OZ011	EG223L	0/40/60	QQSSLLR	RREHLVR	DRTSLAR	3.65	0.23	
OZ012	EG223L	0/40/60	QQSSLLR	RREHLVR	DPTSLNR	4.29	0.38	
			GCA	GCA	GAA			
OZ013	EG223R	50/60/80	SQTQLVR	QSTTLKR	QRNNLGR	10.81	0.41	
OZ014	EG223R	50/60/80	RRQELGR	QGETLKR	QHPNLTR	5.57	0.36	
OZ015	EG223R	50/60/80	RRQELRR	QGGTLNR	QRNNLGR	10.36	1.40	
OZ016	EG223R	50/60/80	RTQELKR	QSGTLKR	QGPNLGR	8.43	0.98	
OZ017	EG223R	50/60/80	NNAQLTR	QSGTLHR	QRPNLGR	6.53	0.55	
OZ018	EG223R	50/60/80	RRQELGR	QGGTLKR	QHPNLTR	9.05	0.42	
OZ019	EG223R	0/60/80	RRQELGR	QSGTLKR	QRNNLGR	9.74	0.73	
OZ020	EG223R	0/60/80	RGVELKR	QSGTLHR	QRPNLTR	11.48	1.63	
OZ021	EG223R	0/60/80	RPQELAR	QSGTLKR	QHPNLTR	8.39	0.46	
OZ022	EG223R	0/60/80	RRQELVR	QSGTLKR	QHPNLTR	9.38	0.62	
OZ023	EG223R	0/60/80	HKGQLNR	QSGTLKR	QRNNLGR	8.74	0.41	
OZ024	EG223R	0/60/80	RQQELDR	QSGTLHR	QHPNLTR	11.92	0.98	
			GGT	GAT	GAA			
OZ025	EG292L	50/40/60	TSTRLMI	LLHNLTR	QRNNLGR	4.40	0.13	
OZ026	EG292L	50/40/60	DKTKLNV	VRHNLTR	QDGNLGR	3.33	0.09	
OZ027	EG292L	50/40/60	TNQKLVV	VAHNLRR	QHPNLTR	4.89	0.81	
OZ028	EG292L	50/40/60	DRPTLRR	QGGNLVR	QGDNLGR	1.10	0.04	
OZ029	EG292L	50/40/60	TRQRLTV	VNHNLTR	LGENLRR	3.69	0.59	
OZ030	EG292L	50/40/60	TNQKLEV	VRHNLQR	QHPNLTR	5.43	0.40	
OZ031	EG292L	0/40/60	TTTKLAI	VRHNLTR	LGENLRR	3.48	1.00	
OZ032	EG292L	0/40/60	TKQRLEV	VPHNLKR	QSVNLRR	4.54	0.67	
OZ033	EG292L	0/40/60	HMSPLRV	QRETLKR	DVGNLGR	1.05	0.22	+
OZ034	EG292L	0/40/60	TSQRLAV	VAHNLRR	QRNNLDR	6.25	1.16	
OZ035	EG292L	0/40/60	RRLALNR	LSQTLKR	AGDNLGR	0.80	0.08	
OZ036	EG292L	0/40/60	TRQRLTV	VRHNLTR	QRNNLGR	5.39	0.87	
			GGC	GAC	GAC			
OZ037	EG292R	50/60/80	APSKLLR	EQGNLLR	DGGNLGR	5.65	0.65	
OZ038	EG292R	50/60/80	APSKLDR	LGENLRR	DGGNLGR	4.74	0.05	
OZ039	EG292R	50/60/80	APSKLDR	LGENLRR	DGGNLGR	5.57	1.03	
OZ040	EG292R	50/60/80	APSKLQV	EKQNLAR	DPSNLRR	7.59	0.53	
OZ041	EG292R	50/60/80	APSKLMR	DKANLTR	DQGNLIR	6.00	0.17	
OZ042	EG292R	0/60/80	APSKLDR	LSENLAR	DPSNLRR	1.53	92.11	
OZ043	EG292R	0/60/80	APSKLDR	DDANLTR	DPSNLRR	0.81	0.16	
OZ044	EG292R	0/60/80	APSKLDR	LGENLAR	DPSNLRR	6.40	1.64	
OZ045	EG292R	0/60/80	APSKLDR	LGENLRR	DPSNLRR	1.38	0.17	
OZ046	EG292R	0/60/80	APSKLDR	DSSNLRR	DQGNLIR	8.40	2.07	
			GCC	GAT	GTC			
OZ047	EG382L	50/40/60	KTTNLKR	LSQTLKR	HAHRLSD	1.06	0.40	
OZ048	EG382L	50/40/60	TNRDLGR	LSENLKR	DPTSLNR	3.39	0.15	
OZ049	EG382L	50/40/60	VRKDLVR	LLHNLTR	DRTPLNR	6.02	0.37	
OZ050	EG382L	50/40/60	HRRDLDR	VAHNLTR	DSSPLTR	5.50	0.28	
OZ051	EG382L	50/40/60	HQRDLMR	VRHNLTR	DPTSLNR	7.93	0.07	
OZ052	EG382L	0/40/60	DSPTLRR	VRHNLTR	DRTSLAR	16.44	1.39	
OZ053	EG382L	0/40/60	DSPTLRR	VRHNLTR	DRTSLAR	13.84	1.53	
OZ054	EG382L	0/40/60	MRRDLDR	VAHNLRR	DPTSLNR	6.90	0.57	
OZ055	EG382L	0/40/60	VRKDLDR	IKENLMR	DRSSLRR	21.18	2.30	
			GGC	GAC	GAG			
OZ056	EG382R	1-step gradient	APSKLDR	DVSNLAR	RRDGLRR	10.15	0.24	
OZ057	EG382R	1-step gradient	APSKLDR	DRGNLTR	RQDLLIR	5.83	0.28	

OZ058	EG382R	1-step gradient	APSKLDR	DSSNLRR	VHWNLMR	9.06	0.25	
OZ059	EG382R	1-step gradient	APSKLDR	LVENLRR	RVENLHR	5.84	1.27	
OZ060	EG382R	1-step gradient	APSKLDR	DGSNLRR	REDNLGR	5.66	0.36	
OZ061	EG382R	1-step gradient	APSKLDR	DASNLAR	VHWNLMR	9.21	0.47	
OZ062	EG382R	1-step gradient	APSKLDR	DRGNLQR	RQDLLIR	6.39	1.12	
OZ063	EG382R	1-step gradient	APSKLDR	DKANLTR	RHDQLTR	5.89	0.33	
OZ064	EG382R	1-step gradient	VPSKLKR	MRENLAR	RIDNLGR	5.20	0.67	
OZ065	EG382R	1-step gradient	APSKLDR	DNANLKR	RRDGLRR	5.37	1.01	
OZ066	EG382R	1-step gradient	APSKLTV	DGSNLAR	RIDNLGR	0.79	0.08	
			GAT	GCG	GTG			
OZ067	EG502L	2-step gradient	TKQHLAV	RMDMLKR	RPDALPR	1.62	0.02	
OZ068	EG502L	2-step gradient	TRQNLDT	RRDTLER	RPDALPR	2.42	0.02	
OZ069	EG502L	2-step gradient	TKQRLVV	RTDTLAR	RPDALPR	2.23	0.49	
OZ070	EG502L	2-step gradient	TNQRLAV	RTDTLAR	RPDALPR	1.88	0.10	
OZ071	EG502L	2-step gradient	TRQNLDT	RRDTLRR	RPDALPR	1.75	0.79	
OZ072	EG502L	2-step gradient	EGNNLAR	RRDDLQR	RGDVLGK	1.33	0.10	
OZ073	EG502L	2-step gradient	TKQRLDV	RTDTLAR	RRDRLGL	2.23	0.14	
OZ074	EG502L	2-step gradient	TKQRLDV	RTDTLAR	RPDALPR	2.02	0.19	
			GGC	GAC	GAG			
OZ075	EG502R	2-step gradient	APSKLMR	DRANLTR	RPDNLPR&	9.47	0.53	
OZ076	EG502R	2-step gradient	SPSKLIR	DGSNLAR	RVDNLPR	10.74	0.53	
OZ077	EG502R	2-step gradient	AQSKLAR	DGSNLRR	RQDGLGS	7.73	1.26	
OZ078	EG502R	2-step gradient	SNSKLAR	DMSNLSR	RTENLTR	5.70	1.08	
OZ079	EG502R	2-step gradient	APSKLDR	DESNLRR	RTSNLTR	10.28	1.61	+
OZ080	EG502R	2-step gradient	APSKLDR	DGSNLRR	RPDNLPR	8.72	0.51	
OZ081	EG502R	2-step gradient	APSKLDR	LQENLAR	VHWNLMR	9.20	0.69	
OZ082	EG502R	2-step gradient	APSKLDR	DESNLRR	RVDNLPR	9.98	1.62	
			GCC	GTC	GCC			
OZ083	EG568L	1-step gradient	SNKDLTR	DHSSLKR	DPSNLRR	2.97	0.41	
OZ084	EG568L	1-step gradient	DSPTLRR	DPSVLKR	EHRGLKR	1.31	0.30	
OZ085	EG568L	1-step gradient	VRKDLDR	DSAVLTR	EHRGLKR	1.11	0.12	
OZ086	EG568L	1-step gradient	DSPTLRR	DREVLRR	ERRALKR	3.99	1.47	
OZ087	EG568L	1-step gradient	HQRDLMR	DSAVLTR	EKRRLAG	1.17	0.28	
OZ088	EG568L	1-step gradient	HNRDLTR	DISVLHR	EKRRLAL	1.03	0.07	
OZ089	EG568L	1-step gradient	VRKDLAR	DREVLRR	DHSNLSR	1.37	0.14	
OZ090	EG568L	1-step gradient	TARALVR	DHSVLKR	ERRGLHR	1.54	0.12	+
OZ091	EG568L	1-step gradient	DRRDLGR	DRGGLRR	EHRGLNR	1.04	0.05	
OZ092	EG568L	2-step gradient	DSPTLRR	RTDGLRR	DHSNLSR	5.49	0.74	
OZ093	EG568L	2-step gradient	DSPTLRR	RTDGLRR	DHSNLSR	5.55	0.85	
OZ094	EG568L	2-step gradient	DSPTLRR	RTDGLRR	DHSNLSR	5.20	1.08	
OZ095	EG568L	2-step gradient	DSPTLRR	RTDGLRR	DHSNLSR	5.65	0.55	
OZ096	EG568L	2-step gradient	DSPTLRR	RTDGLRR	DHSNLSR	5.13	0.15	
OZ097	EG568L	2-step gradient	DSPTLRR	RTDGLRR	DHSNLSR	5.04	0.51	
OZ098	EG568L	2-step gradient	HNTRLAV	DREVLRR	ERRGLAR	0.78	0.15	
			GCC	GCT	GCT			
OZ099	EG568R	2-step gradient	TARALVR	LSQTLKR	LKHDLGR	10.04	2.23	+
OZ100	EG568R	2-step gradient	LKKDLLR	LSQTLNR	LRHDLHR	6.00	0.98	
OZ101	EG568R	2-step gradient	DPSTLRR	LRDSLKR	LGHTLNR	7.01	1.81	
OZ102	EG568R	2-step gradient	DPSTLRR	LRDSLKR	LGHTLNR	7.88	0.86	
OZ103	EG568R	2-step gradient	DPSTLRR	LRDSLKR	LGHTLNR	7.32	1.49	
OZ104	EG568R	2-step gradient	DPSTLRR	LRDSLKR	LGHTLNR	7.62	0.39	
OZ105	EG568R	2-step gradient	HRRDLDR	VAHSLKR	LKHDLRR	2.25	1.63	
OZ106	EG568R	2-step gradient	HRRDLDR	LRDSLKR	LGHTLNR	7.67	0.26	
			GTG	GAA	TTA			
OZ107	CF877L	2-step gradient	RKHILDT	QGGNLVR	QQTGLAA	1.92	0.58	+
OZ108	CF877L	2-step gradient	RKSVLLV	QGGNLVR	QTTGLKS	2.31	0.51	
OZ109	CF877L	2-step gradient	RTSSLKR	RREHLTR	QPTGLTA	2.83	0.20	
OZ110	CF877L	2-step gradient	RNFILQR	QGGNLVR	QVNGLKA	1.61	0.15	+
OZ111	CF877L	2-step gradient	RKGVLRI	QGGNLVR	QQTGLNV	2.20	1.90	+
OZ112	CF877L	2-step gradient	RTSSLKR	RREHLTR	QPTGLTA	2.52	0.55	
OZ113	CF877L	2-step gradient	RKSVLHN	QGGNLVR	QTTGLKS	1.61	0.20	
OZ114	CF877L	2-step gradient	RNFILQR	QGGNLVR	QQTGLAA	2.95	0.18	
OZ115	CF877L	2-step gradient	RNFILQR	QGGNLVR	QVNGLKA	2.71	0.12	
OZ116	CF877L	2-step gradient	RRHVLER	QGGNLVR	QQTGLNV	2.53	0.38	
OZ117	CF877L	2-step gradient	RKSVLLV	QGGNLVR	QQTGLAA	3.87	0.33	
OZ118	CF877L	2-step gradient	RNFILQR	QGGNLVR	QQTGLNV	3.55	0.08	
			GAG	TGG	TTA			

OZ119	CF877R	2-step gradient	RQSNLSR	RKEHLDI	QMTGLNA	2.78	0.35	
OZ120	CF877R	2-step gradient	RQSNLAR	RKEHLVG	QASGLNS	2.53	0.01	
OZ121	CF877R	2-step gradient	RQSNLSR	RKEHLSI	QRTGLTA	2.91	0.19	
OZ122	CF877R	2-step gradient	TTHNLMR	RADHLKV	QGTGLRA	4.72	0.59	
OZ123	CF877R	2-step gradient	TKHNLVR	RREHLNI	QTSGLTA	5.03	0.63	
OZ124	CF877R	2-step gradient	TKHNLVR	RREHLNI	QTSGLTA	4.41	0.20	
OZ125	CF877R	2-step gradient	TKHNLVR	RQEHLNI	QPTGLKV	4.00	0.85	
OZ126	CF877R	2-step gradient	TAHNLMR	RREHLTI	QMTGLNA	2.57	0.28	
OZ127	CF877R	2-step gradient	RMSNLDR	RREHLTI	QGTGLRA	1.60	0.02	
OZ128	CF877R	2-step gradient	TTHNLMR	RKEHLSI	QMTGLNA	2.12	0.07	
OZ129	CF877R	2-step gradient	RQSNLSR	RKEHLDI	QMTGLNA	2.55	0.07	
OZ130	CF877R	2-step gradient	RPHNLLR	RADHLKV	QTTGLNA	2.47	0.22	
OZ131	CF877R	2-step gradient	KHSNLTR	RREHLTI	QPTGLRA	2.08	0.12	
OZ132	CF877R	2-step gradient	RQSNLSR	RSEHLAI	QRVGLHA	1.28	0.05	
OZ133	CF877R	2-step gradient	KHSNLTR	RADHLKV	QNTGLHA	3.24	0.05	
OZ134	CF877R	2-step gradient	RQSNLSR	RNEHLVL	QKTGLRV	3.71	0.19	
OZ135	CF877R	2-step gradient	KHSNLTR	RREHLTI	QMTGLNA	2.25	0.07	
OZ136	CF877R	2-step gradient	KHSNLTR	RREHLTI	QMTGLNA	2.16	0.06	
OZ137	CF877R	2-step gradient	RHSNLTR	RQEHLNI	QMTGLNA	2.26	0.04	
OZ138	CF877R	2-step gradient	KKTNLTR	RREHLTI	QQTGLNV	2.52	0.41	
OZ139	CF877R	2-step gradient	KHSNLTR	RKEHLSI	QMTGLNA	2.74	0.03	
OZ140	CF877R	2-step gradient	KHSNLTR	RKEHLTI	QRTGLSI	2.99	0.48	
OZ141	CF877R	2-step gradient	KHGNLTR	RREHLTI	QQTGLNV	2.87	0.08	
OZ142	CF877R	2-step gradient	KHSNLTR	RKEHLDI	QMTGLNA	2.73	0.16	
			GCT	GAC	GAA			
OZ143	VF2471L	2-step gradient	QRTDLSR	DKGNLSR	QHPNLTR	5.71	0.14	
OZ144	VF2471L	2-step gradient	TKQGLQR	LQENLTR	QHPNLTR	9.95	1.57	
OZ145	VF2471L	2-step gradient	QRQALDR	DNSNLAR	QRNNLGR	6.33	0.14	
OZ146	VF2471L	2-step gradient	GRQALDR	DKANLTR	QRNNLGR	6.85	0.97	
OZ147	VF2471L	2-step gradient	QTADLRR	DSGNLTR	QGPNLSR	6.59	1.69	+
OZ148	VF2471L	2-step gradient	QRQALDR	DNSNLAR	QRNNLGR	5.04	1.01	
OZ149	VF2471L	2-step gradient	TKQGLQR	LQENLTR	QHPNLTR	6.78	0.36	
OZ150	VF2471L	2-step gradient	GRQALDR	DKANLTR	QRNNLGR	5.74	1.02	
OZ151	VF2471L	2-step gradient	TKQGLQR	LPENLTR	QGPNLSR	6.08	1.02	
OZ152	VF2471L	2-step gradient	TKQGLQR	LGENLRR	QRNNLGR	5.79	1.49	
OZ153	VF2471L	2-step gradient	ARQGLNR	DKANLTR	QGPNLSR	6.00	0.34	
OZ154	VF2471L	2-step gradient	TKQGLQR	LRENLAR	QHPNLTR	8.01	0.05	
			GTG	GAC	GAG			
OZ155	VF2471R	2-step gradient	RHTVLRV	DRANLLR	RGDNLNR	8.42	0.60	
OZ156	VF2471R	2-step gradient	RPFTLAR	DRANLLR	RADNLGR	9.19	0.80	
OZ157	VF2471R	2-step gradient	RPFTLAR	DRANLLR	RADNLGR	9.36	0.57	
OZ158	VF2471R	2-step gradient	RNFILQR	DRSNLTR	RHDQLTR	6.84	0.46	
OZ159	VF2471R	2-step gradient	RPFTLAR	DRANLLR	RADNLGR	9.80	1.20	
OZ160	VF2471R	2-step gradient	RSTLLRV	DASNLAR	RGDNLNR	9.22	3.83	
OZ161	VF2471R	2-step gradient	RPFTLAR	DRANLLR	RADNLGR	9.02	0.33	
OZ162	VF2471R	2-step gradient	RKTILTT	DRANLLR	RADNLGR	11.54	0.69	
OZ163	VF2471R	2-step gradient	RNSVLQL	DEGNLSR	RIDNLGR	8.88	0.76	
OZ164	VF2471R	2-step gradient	RASVLDI	DRGNLTR	REDNLGR	6.90	0.24	
OZ165	VF2471R	2-step gradient	RNFILQR	DPSNLAR	RRDGLRR	5.40	0.09	+
OZ166	VF2471R	2-step gradient	RNFILQR	DRANLRR	RHDQLTR	9.67	1.17	
			GGT	GGT	GGA			
OZ167	VF3537L	2-step gradient	LRHHLEA	HNHHLVR	QNSHLRR	5.07	0.60	
OZ168	VF3537L	2-step gradient	LRHHLEA	MKHHLTR	QTTHLRR	4.56	2.10	
OZ169	VF3537L	2-step gradient	LRHHLEA	MSHHLIR	QNSHLRR	5.59	0.12	
OZ170	VF3537L	2-step gradient	LRHHLEA	MKHHLTR	QTTHLRR	4.97	0.18	
OZ171	VF3537L	2-step gradient	TKQKLQV	HNHHLVR	QTDHLKR	5.77	0.44	
OZ172	VF3537L	2-step gradient	MKHHLAR	EAHHLSR	QNSHLRR	5.46	0.96	
OZ173	VF3537L	2-step gradient	LRHHLEA	LPHHLQR	QNSHLRR	5.00	0.79	
OZ174	VF3537L	2-step gradient	RKQHLDA	HNHHLVR	QTTHLRR	7.21	0.53	
OZ175	VF3537L	2-step gradient	LRHHLEA	MKHHLGR	QSQHLKR	3.37	0.07	
OZ176	VF3537L	2-step gradient	MKHHLDA	LPHHLQR	QGGHLAR	5.38	0.09	
OZ177	VF3537L	2-step gradient	LRHHLEA	MSHHLIR	QNSHLRR	6.39	0.32	
OZ178	VF3537L	2-step gradient	LRHHLEA	MSHHLIR	QNSHLRR	4.58	0.15	+
			GGC	GGC	GCC			
OZ179	VF3537R	2-step gradient	RGDHLDR	LKEHLTR	DPSNLRR	14.24	3.89	
OZ180	VF3537R	2-step gradient	RGDHLDR	LKEHLTR	DPSNLRR	8.29	0.66	
OZ181	VF3537R	2-step gradient	RGDHLDR	LKEHLTR	DPSNLRR	5.29	3.37	
OZ182	VF3537R	2-step gradient	APSKLDR	EASKLKR	DPSNLRR	3.28	0.03	
OZ183	VF3537R	2-step gradient	RGDHLDR	LKEHLTR	DPSNLRR	13.74	7.23	

OZ184	VF3537R	2-step gradient	APSKLKR	ERSHLKR	DPSNLRR	1.03	0.11	
OZ185	VF3537R	2-step gradient	APSKLKR	EQSKLVR	DPSNLRR	3.99	0.18	
OZ186	VF3537R	2-step gradient	RGDHLDR	LKEHLTR	DPSNLRR	7.03	5.32	
OZ187	VF3537R	2-step gradient	VPSKLKR	ERSKLKR	DPSNLRR	12.53	0.80	
			GGT	GGA	GGA			
OZ188	VF3540L	2-step gradient	IPNHLAR	QSAHLKR	QNSHLRR	13.95	0.37	
OZ189	VF3540L	2-step gradient	IPNHLAR	QSAHLKR	QNSHLRR	15.08	1.41	
OZ190	VF3540L	2-step gradient	IPNHLAR	QSAHLKR	QNSHLRR	14.09	0.76	
OZ191	VF3540L	2-step gradient	LRHHLEA	QSPHLKR	QGGHLKR	4.09	2.71	
OZ192	VF3540L	2-step gradient	KHSNLTR	RNENLAR	RIDKLGP	4.45	0.32	
OZ193	VF3540L	2-step gradient	IPNHLAR	QSAHLKR	QQAHLAR	12.73	1.36	
OZ194	VF3540L	2-step gradient	IPNHLAR	QSAHLKR	QMSHLKR	15.85	5.11	+
OZ195	VF3540L	2-step gradient	IPNHLAR	QSAHLKR	QNSHLRR	14.00	1.17	
OZ196	VF3540L	2-step gradient	IPNHLAR	QSAHLKR	QAGHLTR	13.06	1.05	
OZ197	VF3540L	2-step gradient	IPNHLAR	QSAHLKR	QQAHLAR	10.80	0.44	
OZ198	VF3540L	2-step gradient	IPNHLAR	QSAHLKR	QQAHLAR	14.31	1.08	
OZ199	VF3540L	2-step gradient	IPNHLAR	QSAHLKR	QQAHLAR	14.58	0.60	+
			GGA	GGC	GGC			
OZ200	VF3540R	2-step gradient	EESNLRR	RPDVLAR	RVDDLGR	15.71	0.65	
OZ201	VF3540R	2-step gradient	EESNLRR	RPDVLAR	RVDDLGR	16.79	1.38	
OZ202	VF3540R	2-step gradient	DEANLRR	RKDDLKR	REDSLPR	8.64	0.32	
OZ203	VF3540R	2-step gradient	DEANLRR	RKDDLKR	REDSLPR	7.92	1.49	
OZ204	VF3540R	2-step gradient	DEANLRR	RKDDLKR	REDSLPR	7.15	0.79	
OZ205	VF3540R	2-step gradient	EESNLRR	RRESLVR	REDSLPR	12.93	0.83	
OZ206	VF3540R	2-step gradient	DEANLRR	RKDDLKR	REDSLPR	10.23	4.44	
OZ207	VF3540R	2-step gradient	EESNLRR	RRESLVR	REDSLPR	11.05	2.29	
OZ208	VF3540R	2-step gradient	DEANLRR	RKDDLKR	REDSLPR	8.34	0.09	
OZ209	VF3540R	2-step gradient	DEANLRR	RKDDLKR	REDSLPR	7.95	0.09	
			GCT	GCT	GAC			
OZ210	VF2468L	2-step gradient	LRQTLAR	VAHSLKR	DPSNLRR	5.98	1.20	
OZ211	VF2468L	2-step gradient	LRQTLAR	VAHSLKR	DPSNLRR	6.68	1.26	
OZ212	VF2468L	2-step gradient	LRQTLAR	VAHSLKR	DPSNLRR	5.93	0.85	
OZ213	VF2468L	2-step gradient	TKQVLDR	VKHSLQR	DPSNLRR	4.38	0.65	
OZ214	VF2468L	2-step gradient	LRQTLAR	VAHSLKR	DPSNLRR	5.68	0.06	
OZ215	VF2468L	2-step gradient	TKQVLDR	VKHSLQR	DPSNLRR	3.63	0.09	
OZ216	VF2468L	2-step gradient	MKNTLTR	QRSDLTR	DPSNLRR	5.47	0.21	
OZ217	VF2468L	2-step gradient	TGQILDR	VAHSLKR	DPSNLRR	7.19	2.15	
OZ218	VF2468L	2-step gradient	LRQTLAR	VAHSLKR	DPSNLRR	6.84	0.43	
OZ219	VF2468L	2-step gradient	GRLALLR	VAHSLKR	DPSNLRR	6.34	0.69	
			GGA	TGA	GAG			
OZ220	VF2468R	2-step gradient	RQDRLDR	QREHLVT	RRDNLNR	9.50	0.19	
OZ221	VF2468R	2-step gradient	RQDRLDR	QKEHLAG	RRDNLNR	9.65	1.51	
OZ222	VF2468R	2-step gradient	RQDRLDR	QKEHLAV	RGDNLKR	10.22	1.00	
OZ223	VF2468R	2-step gradient	RQDRLDR	QNEHLKV	RADNLRR	11.92	3.09	
OZ224	VF2468R	2-step gradient	THAHLTR	QREHLNG	RADNLGR	11.96	1.07	
OZ225	VF2468R	2-step gradient	THAHLTR	QREHLTG	RRDNLNR	11.54	0.52	
OZ226	VF2468R	2-step gradient	RNDRLLR	QKEHLTV	RRDNLNR	11.55	0.53	
OZ227	VF2468R	2-step gradient	RQDRLDR	QKEHLAG	RRDNLNR	11.59	1.15	
OZ228	VF2468R	2-step gradient	THAHLTR	QREHLVT	RRDNLNR	11.69	1.17	
OZ229	VF2468R	2-step gradient	THAHLTR	QNEHLTG	RGDNLAR	10.69	0.51	
OZ230	VF2468R	2-step gradient	THAHLTR	QREHLNG	RGDNLKR	14.10	0.15	
OZ231	VF2468R	2-step gradient	THAHLTR	QREHLVT	RIDNLGR	12.63	1.65	
			GAG	GAG	GGG			
OZ232	VF3542L	2-step gradient	KLTNLTR	REDNLDR	RIDKLGG	4.80	0.39	
OZ233	VF3542L	2-step gradient	RQMNLDR	RQDNLGR	RIDKLGG	5.88	1.39	
OZ234	VF3542L	2-step gradient	KHHNLLR	RDDNLQR	RMEHLPR	5.22	0.47	
OZ235	VF3542L	2-step gradient	KPSNLER	RPDNLVR	RIDKLGG	6.10	0.22	
OZ236	VF3542L	2-step gradient	KHSNLTR	RADNLGR	RMEHLPR	4.44	0.41	
OZ237	VF3542L	2-step gradient	KQSNLLR	REDNLDR	RRHGLGR	4.71	0.60	
OZ238	VF3542L	2-step gradient	RMSNLDR	REDNLGR	RDDGLGR	3.13	0.12	
OZ239	VF3542L	2-step gradient	RASNLTR	REDNLDR	RRWGLGR	4.38	0.40	
OZ240	VF3542L	2-step gradient	KHSNLTR	RDDNLQR	RNDKLVP	5.18	0.45	
			GAC	GCG	GCG			
OZ241	VF3542R	2-step gradient	EEANLRR	RRDDLTR	REDVLGR	8.53	1.23	
OZ242	VF3542R	2-step gradient	EEANLRR	RSDDLRR	RLDMLAR	8.72	1.11	
OZ243	VF3542R	2-step gradient	EESNLRR	RRDDLTR	RLDMLAR	11.42	0.12	
OZ244	VF3542R	2-step gradient	EESNLRR	RRDDLTR	RLDMLAR	13.12	1.53	

OZ245	VF3542R	2-step gradient	EEANLRR	RRDDLTR	RLDMLAR	9.96	0.16	
OZ246	VF3542R	2-step gradient	EESNLRR	RRDDLTR	RKDLLHR	10.16	0.55	
OZ247	VF3542R	2-step gradient	EQSNLRR	RRDDLTR	RLDMLAR	8.42	1.54	
OZ248	VF3542R	2-step gradient	EESNLRR	RRDDLTR	RLDMLAR	12.11	0.66	
OZ249	VF3542R	2-step gradient	EESNLRR	RRDDLLR	RIDNLGR	12.25	0.70	
OZ250	VF3542R	2-step gradient	EEANLRR	RRDDLTR	RTDLLGR	8.98	0.60	
OZ251	VF3542R	2-step gradient	EEANLRR	RRDDLTR	RLDMLAR	10.25	1.46	
OZ252	VF3542R	2-step gradient	EEANLRR	RKEDLAR	RLDMLAR	11.82	0.37	
			GGC	GCC	GCC			
OZ253	VF3552L	2-step gradient	VPSKLLR	DPSVLTR	EHRGLKR	4.29	0.30	
OZ254	VF3552L	2-step gradient	TPSKLLR	DPSVLTR	EHRGLKR	7.39	1.10	
OZ255	VF3552L	2-step gradient	SNSKLDR	DPSVLTR	EHRGLKR	3.30	0.23	
OZ256	VF3552L	2-step gradient	SPSKLVR	DPSVLTR	EGGTLRR	2.88	0.10	+
OZ257	VF3552L	2-step gradient	SPSKLVR	DPSVLTR	EHRGLKR	3.22	0.15	
OZ258	VF3552L	2-step gradient	TPSKLLR	DSSVLRR	ERRGLAR	33.85	27.58	
OZ259	VF3552L	2-step gradient	TPSKLLR	DSSVLRR	ERRGLAR	20.62	20.68	
OZ260	VF3552L	2-step gradient	SPSKLVR	DSSVLRR	ERRGLAR	14.89	11.80	
OZ261	VF3552L	2-step gradient	TPSKLLR	DSSVLRR	ERRGLAR	49.72	42.09	
OZ262	VF3552L	2-step gradient	VPSKLLR	DPSVLTR	EHRGLKR	4.30	0.30	
			GCG	GAC	GTG			
OZ263	VF3552R	2-step gradient	KHDTLHR	DRGNLTR	RGDALAR	36.42	20.49	
OZ264	VF3552R	2-step gradient	KNDTLAR	DRANLRR	RPDALSR	8.12	0.82	
OZ265	VF3552R	2-step gradient	KNDTLAR	DRANLRR	RPDALSR	8.03	1.21	
OZ266	VF3552R	2-step gradient	KHDTLHR	DRGNLTR	RGDALAR	29.45	48.83	
OZ267	VF3552R	2-step gradient	KKHTLVK	LRENLAR	RMDALMR	30.79	5.40	
OZ268	VF3552R	2-step gradient	KNDTLAR	DNSNLAR	RGDALAR	3.93	0.17	
OZ269	VF3552R	2-step gradient	KKHTLTK	DRGNLQR	RGDALAR	9.93	2.89	
OZ270	VF3552R	2-step gradient	RNHTLAR	DNSNLAR	RGDALAR	4.67	4.12	
OZ271	VF3552R	2-step gradient	KNDTLAR	ESGNLAR	RGDVLGK	8.83	0.45	
OZ272	VF3552R	2-step gradient	RSDTLAR	DQGNLRR	RPDALPR	10.32	1.44	
OZ273	VF3552R	2-step gradient	KRHTLTR	DSGNLTR	RLDVLGN	3.91	0.48	
			GGG	GCT	GCC			
OZ274	HX508L	2-step gradient	RSAHLQA	LSQTLKR	ERRGLAR	2.12	0.23	
OZ275	HX508L	2-step gradient	RSAHLQA	LSQTLKR	EHRGLKR	3.43	0.23	
OZ276	HX508L	2-step gradient	RSAHLQA	LSQTLKR	EHRGLKR	6.31	2.17	+
OZ277	HX508L	2-step gradient	RGEHLTN	LSQTLKR	EHRGLKR	3.61	0.72	
OZ278	HX508L	2-step gradient	RSAHLQA	LSQTLKR	DPSNLRR	2.75	0.15	
OZ279	HX508L	2-step gradient	RRLHLTN	LSQTLKR	DPSNLRR	1.89	0.04	
OZ280	HX508L	2-step gradient	RRLHLTN	LSQTLKR	DPSNLRR	2.34	0.13	
			GCC	GAT	GCT			
OZ281	HX508R	2-step gradient	AKRDLDR	LMHNLTR	LKHDLRR	5.74	0.65	
OZ282	HX508R	2-step gradient	HRRDLDR	LMHNLTR	LKHDLRR	7.92	0.93	
OZ283	HX508R	2-step gradient	AKRDLDR	LLHNLTR	LKHDLRR	4.79	0.37	
OZ284	HX508R	2-step gradient	DGSTLNR	VRHNLTR	VQNSLTR	8.53	1.36	
OZ285	HX508R	2-step gradient	DGSTLNR	IRHNLTR	LKHDLRR	6.19	0.18	
OZ286	HX508R	2-step gradient	AKRDLDR	LLHNLTR	LKHDLRR	4.87	0.45	
OZ287	HX508R	2-step gradient	LKKDLLR	IKHNLAR	LKHDLRR	14.03	4.08	
OZ288	HX508R	2-step gradient	DSSTLAR	VRHNLTR	LKHDLRR	2.92	1.96	
OZ289	HX508R	2-step gradient	DGSTLRR	VRHNLTR	VSNSLAR	5.88	0.19	
OZ290	HX508R	2-step gradient	AKRDLDR	VNHNLTR	LKHDLRR	9.20	4.01	
OZ291	HX508R	2-step gradient	DGSTLNR	VRHNLTR	LKHDLRR	15.46	14.60	
			GGG	GCT	GCG			
OZ292	HX761L	2-step gradient	KQDHLTK	LSQTLKR	RLDMLAR	8.12	2.53	
OZ293	HX761L	2-step gradient	KQDHLTK	LSQTLKR	RLDVLAR	5.32	2.71	
OZ294	HX761L	2-step gradient	KQDHLRV	LSQTLKR	RPDGLAR	14.19	1.10	
OZ295	HX761L	2-step gradient	KKDHLHR	LSQTLKR	RLDMLAR	13.99	1.72	
OZ296	HX761L	2-step gradient	KQDHLRV	LSQTLKR	RPDGLAR	13.85	4.18	
OZ297	HX761L	2-step gradient	KQDHLTK	LSQTLKR	RLDMLAR	10.47	2.07	
OZ298	HX761L	2-step gradient	KQDHLTK	LSQTLKR	RLDMLAR	11.51	0.66	
OZ299	HX761L	2-step gradient	KQDHLRV	LSQTLKR	RLDMLAR	9.86	0.62	
OZ300	HX761L	2-step gradient	KKDHLHR	LSQTLKR	RLDMLAR	14.09	0.79	
OZ301	HX761L	2-step gradient	KKDHLHR	LSQTLNR	RLDMLAR	11.23	0.76	
OZ302	HX761L	2-step gradient	KKDHLHR	LSQTLNR	RLDMLAR	6.65	1.55	
			GCC	TTT	GAG			
OZ303	HX761R	2-step gradient	AKRDLDR	SPNGLII	VHWNLKR	4.07	0.06	
OZ304	HX761R	2-step gradient	DRRGLVR	SPNGLQV	SASNLTR	3.31	0.58	
OZ305	HX761R	2-step gradient	AKRDLDR	SPNGLII	VHWNLKR	4.01	0.20	

OZ306	HX761R	2-step gradient	AKRDLDR	SPNGLEI	VHWNLMR	3.32	0.02	
OZ307	HX761R	2-step gradient	AKRDLDR	SPNGLII	VHWNLKR	3.53	0.49	
OZ308	HX761R	2-step gradient	LKKDLLR	SQLGLQV	SASNLHR	2.44	0.07	+
OZ309	HX761R	2-step gradient	MRRDLLR	SQLGLSV	SASNLTR	2.67	0.05	+
OZ310	HX761R	2-step gradient	MRRDLER	SPNGLVI	VHWNLMR	2.92	0.08	
OZ311	HX761R	2-step gradient	MRRDLLR	SQLGLSV	SASNLTR	2.81	0.44	+
OZ312	HX761R	2-step gradient	AKRDLDR	SPNGLVI	VHWNLMR	3.63	0.17	
OZ313	HX761R	2-step gradient	MRRDLLR	SQLGLSV	SASNLTR	2.55	0.38	+
OZ314	HX761R	2-step gradient	MRRDLLR	SQLGLSV	SASNLTR	2.94	0.14	+
			GGT	GCT	GTG			
OZ315	HX500L	2-step gradient	RQQKLDT	LSQTLKR	RGDALAR	2.76	0.13	
OZ316	HX500L	2-step gradient	TTTKLAI	LSQTLKR	RGDVLGK	2.88	0.55	
OZ317	HX500L	2-step gradient	TTTKLAI	LSQTLKR	RGDVLGK	3.48	0.71	
OZ318	HX500L	2-step gradient	RRSRLDV	LSQTLKR	RGDALAR	3.15	0.06	
OZ319	HX500L	2-step gradient	TTTKLAI	LSQTLKR	RGDVLGK	4.10	0.16	
OZ320	HX500L	2-step gradient	TTTKLAI	LSQTLKR	RGDVLGK	3.86	0.19	+
OZ321	HX500L	2-step gradient	TNQKLQV	LSQTLRR	RGDALAR	3.11	0.11	
OZ322	HX500L	2-step gradient	RQQKLDT	LSQTLKR	RGDVLGK	2.90	0.50	
OZ323	HX500L	2-step gradient	TTTKLAI	LSQTLKR	RGDVLGK	4.09	0.22	+
OZ324	HX500L	2-step gradient	TTTKLAI	LSQTLNR	RGDVLGK	4.93	0.40	
OZ325	HX500L	2-step gradient	TTTKLAI	LSQTLNR	RGDVLGK	5.65	1.02	
			TAC	GCC	GGC			
OZ326	HX500R	2-step gradient	DPSNLIR	DSAVLTR	RKEPLGR	0.96	0.06	
OZ327	HX500R	2-step gradient	PLARLEE	DRSVLRN	KRVSLQG	1.11	0.22	
OZ328	HX500R	2-step gradient	VRSPLPD	DVSVLRR	KRVSLGA	0.96	0.04	
OZ329	HX500R	2-step gradient	PLARLEE	DRSVLKR	KRVSLQG	1.40	0.17	
OZ330	HX500R	2-step gradient	SRLGLVA	DHSVLKR	KNISLNH	1.01	0.27	
OZ331	HX500R	2-step gradient	PLARLEE	DHTVLRR	KRVSLQG	0.93	0.04	
OZ332	HX500R	2-step gradient	DRSNLRK	DRTTLKR	DGGHLSR	1.19	0.01	+
			GCA	GTG	TGG			
OZ333	HX587L	2-step gradient	NKTDLGR	RMDVLTR	RSDHLSL	5.73	0.16	+
OZ334	HX587L	2-step gradient	NKTDLGR	RMDVLTR	RSDHLSL	4.87	0.54	+
OZ335	HX587L	2-step gradient	NKTDLGR	RMDVLTR	RSDHLSL	5.15	0.34	+
OZ336	HX587L	2-step gradient	NKTDLGR	RMDVLTR	RSDHLSL	5.40	0.35	+
OZ337	HX587L	2-step gradient	NKTDLGR	RMDVLTR	RSDHLSL	4.94	0.29	+
OZ338	HX587L	2-step gradient	NKTDLGR	RMDVLTR	RSDHLSL	5.00	0.52	+
OZ339	HX587L	2-step gradient	NKTDLGR	RADSLGR	RADHLPQ	2.51	0.33	
OZ340	HX587L	2-step gradient	NKTDLGR	RRDMLRR	RMDHLAG	14.45	2.74	
OZ341	HX587L	2-step gradient	NKTDLGR	RADSLGR	RADHLPQ	3.10	0.16	
OZ342	HX587L	2-step gradient	TPTDLNR	RRDTLRR	RMDHLAG	5.49	0.17	
OZ343	HX587L	2-step gradient	NKTDLGR	RADSLGR	RADHLPQ	3.34	0.22	
OZ344	HX587L	2-step gradient	LKHGLLR	RKDGLMR	RSEHLGI	3.55	0.33	
			GCC	GGT	TGG			
OZ345	HX587R	2-step gradient	DESTLRR	MKHHLGR	RSDHLSL	8.15	0.73	
OZ346	HX587R	2-step gradient	AKKDLRR	LRQHLVR	RSDHLSL	2.32	0.32	
OZ347	HX587R	2-step gradient	LKKDLLR	LRQSLTR	RSDHLSL	3.10	0.99	
OZ348	HX587R	2-step gradient	VRKDLDR	MKHHLGR	RSDHLSL	4.05	0.12	+
OZ349	HX587R	2-step gradient	SKKSLTR	EAHHLSR	RSDHLSL	7.00	0.27	+
OZ350	HX587R	2-step gradient	DPSTLRR	LPHHLQR	RMDHLAG	4.66	0.64	
OZ351	HX587R	2-step gradient	LAKDLVR	HKHRLVT	RSDHLSL	3.74	0.29	
OZ352	HX587R	2-step gradient	SKKSLTR	QAHILKR	RSDHLSL	7.03	0.64	
OZ353	HX587R	2-step gradient	HRRDLDR	QRHHLVR	RSDHLSL	4.60	0.16	+
OZ354	HX587R	2-step gradient	DPSTLRR	LPHHLKR	RSDHLSL	7.25	0.16	+
OZ355	HX587R	2-step gradient	MRRDLLR	LGHHLVR	RSDHLSL	3.94	0.27	
OZ356	HX587R	2-step gradient	DPSTLRR	QTHHLQR	RSDHLSL	4.48	0.33	
			TCT	GAG	TGG			
OZ357	HX735L	2-step gradient	SKPNLKM	RQDNLGR	RMDHLAG	3.58	0.69	
OZ358	HX735L	2-step gradient	SKPNLKM	RQDNLGR	RSDRLAL	2.29	0.12	+
OZ359	HX735L	2-step gradient	SKPNLKM	RADNLGR	RSDRLAL	2.20	0.47	+
OZ360	HX735L	2-step gradient	SKPNLKM	RADNLGR	RSDRLAL	2.32	0.21	
OZ361	HX735L	2-step gradient	TKPNLKI	RGDNLVR	RSDHLSL	2.84	0.36	+
OZ362	HX735L	2-step gradient	SKPNLKM	RQDNLGR	RRDRLRI	2.63	0.28	
OZ363	HX735L	2-step gradient	SKPNLKM	RGDNLGR	RSDHLSL	3.01	0.12	+
OZ364	HX735L	2-step gradient	SNRNLKT	RQDNLGR	RKAGLHI	2.56	0.67	
OZ365	HX735L	2-step gradient	TKPLLKI	RQDNLGR	RSDRLAL	1.70	0.09	
OZ366	HX735L	2-step gradient	SNRNLRI	RADNLGR	RSDRLAL	1.96	0.14	
			GAG	GAA	GGG			

OZ367	HX735R	2-step gradient	KHSNLTR	QGANLVR	RNDKLVP	4.85	0.88	+
OZ368	HX735R	2-step gradient	KLTNLTR	QKVNLAR	RIDKLGG	4.72	1.15	
OZ369	HX735R	2-step gradient	KHSNLTR	QHTNLTR	RIDKLGG	5.51	0.94	+
OZ370	HX735R	2-step gradient	KKTNLTR	QMSNLDR	RIDKLGG	6.88	1.22	
OZ371	HX735R	2-step gradient	KLTNLTR	QMSNLDR	RGDKLGH	4.65	1.24	
OZ372	HX735R	2-step gradient	KHSNLTR	QRVNLAR	RIDKLGG	4.13	0.92	
OZ373	HX735R	2-step gradient	KHSNLTR	QKVNLAR	RGDKLGP	5.25	0.52	
OZ374	HX735R	2-step gradient	KHSNLTR	QLANLGR	RIDKLGG	4.66	0.53	+
OZ375	HX735R	2-step gradient	KHSNLTR	QKVNLAR	RGDKLGP	4.53	0.96	
OZ376	HX735R	2-step gradient	RQSNLSR	QMSNLDR	RIDKLGG	4.90	1.80	+
OZ377	HX735R	2-step gradient	KHSNLTR	QQTNLAR	RGDKLGP	5.59	0.65	
			GCT	GGC	TCT			
OZ378	HX2119L	2-step gradient	HRPSLVR	ERGHLTR	QRNALAG	1.22	0.02	
OZ379	HX2119L	2-step gradient	KHQTLQR	ERGHLNR	QRNALAG	1.26	0.37	
OZ380	HX2119L	2-step gradient	ATGDLRR	ENSGLKR	QNNALTG	1.01	0.30	
OZ381	HX2119L	2-step gradient	AKQGLRR	LKEHLTR	QRNTLQG	1.41	0.06	+
OZ382	HX2119L	2-step gradient	RSLTLLR	EQSKLTR	ARNLLRG	0.77	0.05	
OZ383	HX2119L	2-step gradient	TKQVLDR	ENSKLKR	QRNALAG	1.46	0.38	
OZ384	HX2119L	2-step gradient	NKQALDR	LHENLKR	QRNALAG	2.47	0.42	
OZ385	HX2119L	2-step gradient	HKLTLVR	ERGHLIR	QRNTLKG	2.69	1.12	
OZ386	HX2119L	2-step gradient	GMLALRR	LHENLKR	ARNALGG	0.95	0.08	
			TTC	GGT	TCT			
OZ387	HX2119R	2-step gradient	RPSHLVT	EAHHLGR	ARHLLKG	1.28	0.21	
OZ388	HX2119R	2-step gradient	LHKLLVI	EPHHLMR	QRNALAG	0.71	0.05	
OZ389	HX2119R	2-step gradient	RENHLRI	ERHQLVR	QRNALGG	0.92	0.04	+
OZ390	HX2119R	2-step gradient	RHHHLDV	EKHQLIR	QRNTLKG	1.41	0.29	
			TTC	GGA	GAA			
OZ391	SR2163L	2-step gradient	RPNHLAI	QSPHLKR	QSNNLTR	8.40	0.29	
OZ392	SR2163L	2-step gradient	RPNHLTA	QSAHLKR	LGENLRR	5.74	0.34	
OZ393	SR2163L	2-step gradient	RPNHLAI	QSPHLKR	QSNNLTR	8.10	0.05	
OZ394	SR2163L	2-step gradient	RANHLTI	QSAHLKR	LGENLRR	6.41	0.87	
			GAT	GGA	GGC			
OZ395	SR2163R	2-step gradient	SQQALGV	QSAHLKR	ESGHLKR	1.70	0.23	
OZ396	SR2163R	2-step gradient	TKQHLAV	QSAHLKR	ESGHLRR	1.89	0.04	+
OZ397	SR2163R	2-step gradient	SKQALAV	QSAHLKR	ENSKLRR	1.89	0.13	+
OZ398	SR2163R	2-step gradient	TNQRLDV	QNPHLTN	KNVSLVG	0.89	0.02	
OZ399	SR2163R	2-step gradient	SKQALAV	QSAHLKR	ENSKLRR	1.74	0.07	+
OZ400	SR2163R	2-step gradient	TKQHLAV	QSAHLKR	ESGHLRR	2.08	0.25	+
OZ401	SR2163R	2-step gradient	SKQALAV	QSAHLKR	ESGHLKR	1.75	0.15	

Table S2

Full ZFN site name	Full ZFN site sequence	Half-site name	Half-site sequence	# of GXX triplets	Successful B2H selection?	Arrays converted to ZFNs	ZFN Pair A	ZFN Pair B	ZFN Pair C	ZFN Pair D
EG223	cTACCCCGACcacatGAAGCAGCAc	EG223L	gGTCGGGGTAg	3	YES	OZ001	X	X		
						OZ009			X	X
		EG223R	tGAAGCAGCAc	3	YES	OZ013	X		X	
						OZ017		X		X
EG292	cACCATCTTCttcaagGACGACGGCa	EG292L	aGAAGATGGTg	3	YES	OZ030	X	X		
						OZ034			X	X
		EG292R	gGACGACGGCa	3	YES	OZ039	X		X	
						OZ044		X		X
EG382	gGGCATCGACttcaagGAGGACGGCa	EG382L	aGTCGATGCCc	3	YES	OZ051	X	X		
						OZ052			X	X
		EG382R	gGAGGACGGCa	3	YES	OZ059	X		X	
						OZ060		X		X
EG502	gATCCGCCACaacatcGAGGACGGCa	EG502L	tGTGGCGGATa	3	YES**	OZ068	X	X		
						OZ069			X	X
		EG502R	cGAGGACGGCa	3	YES	OZ076	X		X	
						OZ082		X		X
EG568	cGGCGACGGCcccgtGCTGCTGCCc	EG568L	gGCCGTCGCCg	3	YES	OZ086	X	X		
						OZ092			X	X
		EG568R	tGCTGCTGCCc	3	YES	OZ099	X		X	
						OZ102		X		X
CF877	tCACTTCTAAtggtgaTTATGGGAGa	CF877L	aTTAGAAGTGa	**2**	YES	OZ118	X			
		CF877R	aTTATGGGAGa	**1**	YES	OZ134	X			
VF2471	cAGCGTCTTCgagagtGAGGACGTGt	VF2471L	cGAAGACGCTg	3	YES	OZ146	X	X		
						OZ154			X	X
		VF2471R	tGAGGACGTGt	3	YES	OZ162	X		X	
						OZ166***		X		X
VF3537	tACCACCTCCTcccccgGCCGGCGGCg	VF3537L	aGGAGGTGGTa	3	YES	OZ172	X	X		
						OZ177			X	X
		VF3537R	gGCCGGCGGCg	3	YES	OZ182	X		X	
						OZ185		X		X
VF3540	cACCTCCTCCccggccGGCGGCGGAc	VF3540L	gGGAGGAGGTg	3	YES	---				
		VF3540R	cGGCGGCGGAc		NO	---				

Table S2

VF2468	gAGCAGCGTCttcgaGAGTGAGGAc	VF2468L	aGACGCTGCTc	3	YES	OZ211	X	X		
						OZ217			X	X
		VF2468R	aGAGTGAGGAc	**2**	YES	OZ227	X		X	
						OZ230		X		X
VF3542	cCTCCTCCCCggccgGCGGCGGACa	VF3542L	cGGGGAGGAGg	3	YES	OZ233	X	X		
						OZ234			X	X
		VF3542R	gGCGGCGGACa	3	YES	OZ244	X		X	
						OZ246		X		X
VF3552	gGCCGGCGGCggacaGTGGACGCGg	VF3552L	cGCCGCCGGCc	3	YES	OZ253	X	X		
						OZ254			X	X
		VF3552R	aGTGGACGCGg	3	YES	OZ264	X		X	
						OZ272		X		X
HX508	aCCCAGCGGCgcctacGCTGATGCCt	HX508L	cGCCGCTGGGt	3	YES	OZ276	X	X		
						OZ277			X	X
		HX508R	cGCTGATGCCt	3	YES	OZ284	X		X	
						OZ285		X		X
HX761	cCCCAGCCGCccccactGAGTTTGCCt	HX761L	gGCGGCTGGGg	3	YES	OZ297	X	X		
						OZ300			X	X
		HX761R	tGAGTTTGCCt	**2**	YES	OZ303	X		X	
						OZ304		X		X
HX500	gACCAGCCACccagcGGCGCCTACg	HX500L	gGTGGCTGGTc	3	YES	---				
		HX500R	cGGCGCCTACg	**2**	NO	---				
HX587	aTGCCACCCAtgcccTGGGGTGCCc	HX587L	aTGGGTGGCAt	**2**	YES	OZ338	X	X		
						OZ340			X	X
		HX587R	cTGGGGTGCCc	**2**	YES	OZ345	X		X	
						OZ349		X		X
HX735	gAGACTCCCAcggccGGGGAAGAGt	HX735L	gTGGGAGTCTc	**1**	YES	OZ357	X	X		
						OZ363			X	X
		HX735R	cGGGGAAGAGt	3	YES	OZ370	X		X	
						OZ371		X		X
HX2119	gAGCGCCAGAttaccaTCTGGTTTCa	HX2119L	aTCTGGCGCTc	**2**	NO	---				
		HX2119R	aTCTGGTTTCa	**1**	NO	---				
SR2163	gGAATCCTTCtaatgaGGCGGAGATc	SR2163L	aGAAGGATTCc	**2**	YES	OZ391	X			
		SR2163R	aGGCGGAGATc*	3	YES**	OZ396	X			

Table S2

Notes:

*This site contained a *dam* methylation site (GATC) and therefore the 3′ most C was mutated in the B2H selection strain and B2H reporter strain.

**Although these arrays failed to activate transcription by more than three-fold in the quantitative B2H assay, they were deemed to be successful because their reporters possessed a high basal level of transcription which can often mask a higher true fold-activation.

***A PCR-induced mutation was introduced into this array when it was transferred to the human ZFN expression vector (a Thr→Ala mutation at position 8 of its F1 recognition helix).

Table S3

Primer Name	Sequence
OK61	5’-GGGTAGTACGATGACGGAACCTGTC-3’
OK1424	5’-GAGCGCCCCTTCCAGTGTCGC-3’
OK1425	5’-CGCATACAGATCCGACACTGAAACGG-3’
OK1426	5’-GTGTCGGATCTGTATGCGAAATTTCTCC-3’
OK1427	5’-TCGGCATTGGAATGGCTTCTCG-3’
OK1428	5’-GCCATTCCAATGCCGAATATGCA-3’
OK1429	5’-CCCTCAGGTGGGTTTTTAGGTG-3’
OK1430	5’-GGGGAGCGCCCCTTCCAGTGTCGC-3’
OK1432	5’-GTGCAGAGGATCCCCTCAGGTGGGTTTTTAGGTG-3’
OK1681	5’-GGCTCTCTGTACATGAAGCAACTCC-3’
OK1682	5’-TCACAGCCTGAAAATTACCCATCC-3’
OK1706	5’CCCTCTCCTCTTCCTTCTCTTCTT-3’
OK1711	5’-GTGCCCCTTCTCTGTCAACCTCTAT-3’
OK1713	5’-GCATGCTTTGATGACGCTTCTGTA-3’
OK1718	5’GATTGCTCTACTTCCCCAAATCACTG-3’
OK1733	5’-GGATGGAGCCAAGGATATCGAAG-3’
OK1734	5’-GTAACTGGCCATAGGCTGGTAGGTT-3’
OK1736	5’-TACGCTGATGCCTGCTGTCAACTAT-3’
OK1738	5’-ACTGTCCACAGGCAACAGGGAGT-3’
OK1773	5’-GAGAGCCGTTCCCTCTTTG-3’
OK1776	5’-GGAAGATGTGGAGAGTTGGAGGAAA-3’
OK1777	5’-CGACTTCTCTCTGGAGCTCTTGCTA-3’
OK1823	5’-AAGTCAAGTTGTTCAGGGGGCTAAG-3’
OK1824	5’-AAGCCACTAACTTTCCTCCTTGTGC-3’
OK1838	5’-AGGGGAGGCATTAGATTCAAGTCAG-3’
OK1845	5’GATTCAACCAGACAGATAGAAGG-3’
OK1846	5’-TTACTGTCTCATCCTTTACTCC-3’
OS216	5'-GAAGGCAAACTCAGTGGGGCGGC-3’
DVO4429	5’-TTTCAGTTTCGTGGCGCTCTCGTC-3’
DVO4444	5’-CCATCTCCCTCTTCTTCCGC-3’
DVO4445	5’-GCGGCGGCTCCATCTCCCTC-3’
DVO4461	5’-GATAATACAAGGCCTAGAACTAGCTCTGTAGC-3’
DVO4462	5’-GTGATGGCAGTTTCATCATGAATG-3’
DVO4565	5’-CCCCTTTTTAGCTTAGTAGTGCTCTCATG-3’
T3 (Invitrogen)	5’-ATTAACCCTCACTAAAGGGA-3’
M13 (Invitrogen)	5’-CAGGAAACAGCTATGAC-3’